Magnetic Field and Magnetic Isotope Effects on the Products of Organic Reactions

IAN R. GOULD, NICHOLAS J. TURRO and
MATTHEW B. ZIMMT

Department of Chemistry, Columbia University, New York, U.S.A.

1 Introduction

ORIGIN OF MAGNETIC FIELD EFFECTS

The effects of magnetic fields on chemical reactions have been the subject of several review articles in recent years (Atkins, 1976; Atkins and Lambert, 1975; Sagdeev *et al.*, 1977b; Lawler and Evans, 1971; Turro and Kraeutler, 1980; Turro, 1983). It is the object of the present review to describe the current theory and to illustrate, with examples, the changes that arise in the formation of products of organic reactions as a function of applied field and of nuclear magnetic spins.

Sporadic reports of magnetic field effects on chemical reactions have appeared for almost 80 years. However, early work was plagued by non-reproducible effects and retractions. The early work is summarized by Atkins and Lambert (1975). Recently, reports of magnetic field effects on chemical reactions have become more widespread and better documented. These reports have been coincident with the observation and subsequent theoretical development of chemically induced magnetic polarization, CIDNP (Kaptein, 1975; Closs, 1971; Buchachenko and Zhidomirov, 1971; Frith and McLauchlan, 1975; Lawler, 1972). Prior to these recent developments, it had been thought that there was no possibility of observing significant magnetic effects on the products of chemical reactions. Based on a simple thermodynamic argument, it can be shown that a very strong magnetic field (100,000 G) can induce an energy change of at most c. 0.03 kcal mol^{-1} even in paramagnetic molecules (Atkins, 1976). Since this energy is negligible compared to commonly encountered activation energies (~ 10 kcal mol^{-1}) it could be concluded that no effect should be observed. However, the rates of chemical reactions depend upon both energetic and entropic factors. Substantial magnetic field effects on reaction probabilities are possible if the effect of the field is to change the number of degrees of freedom open to a chemical system, i.e. affect the factor A in (1) and thus k (Turro and Kraeutler, 1980; Turro, 1983). Specifically, observation of magnetic field effects depends

$$k = (Ae^{-\Delta E/RT}) \qquad (1)$$

upon the system possessing states which have different magnetic properties (e.g. singlet and triplet states). If the application of a magnetic field can either shut off or enhance selected reaction channels for these states, then an effect on the product distribution becomes possible.

A deeper insight into the origin of magnetic effects lies in a description of the electronic and nuclear spin states of a system, and in an understanding of possible magnetic interactions. The bulk of the observations described in the present review are concerned with the reactions of radical pairs and thus we will examine the spin states of radical pair systems as archetypes.

RADICAL PAIR SYSTEMS

An introductory account of this topic has been given by Turro (1978a). Homolytic cleavage of a single bond leads to two one-electron fragments, i.e. radicals; the two radicals constitute a radical pair. If the molecule cleaves from the singlet state (most common for thermal reactions), then the resulting radical pair will be in a singlet state, since the process of bond cleavage is three to four orders of magnitude faster than any mechanism which interconverts the radical pair spin states. Similarly, if the molecule

cleaves from a triplet state (commonly encountered in photochemical processes), then the radical pair will initially be in a triplet state.

Vector spin description of radical pairs

The simultaneous occurrence of charge and spin motion imbues an electron with a magnetic moment. In the presence of a laboratory magnetic field, which is strong compared to molecular magnetic fields, the electron moment of a radical will interact with the applied field. The electron spin can be represented by an angular momentum vector, with the direction of applied field, H, as the positive z-axis. Then, the electron spin vector has a component of angular momentum along the field direction that is either $+1/2\hbar$ (α, parallel) or $-1/2\hbar$ (β, antiparallel) (Fig. 1). The Uncertainty Principle dictates that the spin vector also has a component that is perpendicular to and that precesses about the field direction.
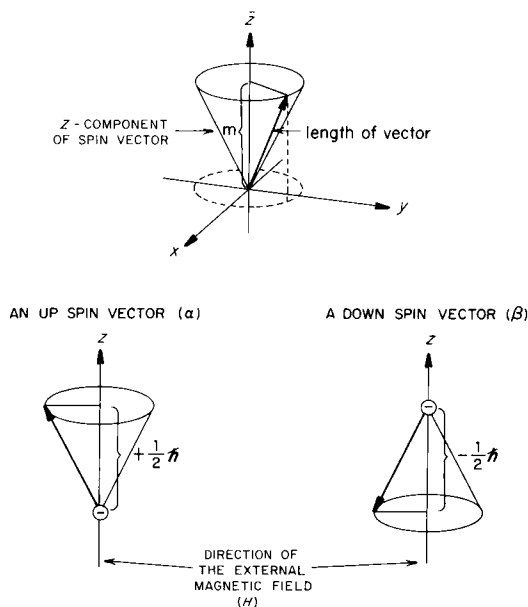
FIG. 1   Vector representation of an electron's spin moment. In the presence of an external magnetic field (H, z-axis) the moment precesses around the axis, which corresponds to the direction of that field. Two orientations of the vector are allowed; an up (α) orientation and a down (β) orientation

In a radical pair the vectors corresponding to the spin of each electron exhibit the same behaviour as those of a single electron. Quantum mechanics dictates, however, that only specific interactions of the two spin vectors may

occur in the initially formed pair (Fig. 2). If formed from a singlet state, the spin vectors of electrons 1 and 2 ($\mathscr{S}_1$ and $\mathscr{S}_2$) must be aligned so that one spin is α, one spin is β, ($M_s = 0$), and their components perpendicular to the field must be 180° out of phase ($S = 0$): a state of zero total spin angular momentum. If formed from a triplet state, three possible interactions may occur, each of which has the spin vectors in phase (0° separation of the perpendicular components, $S = 1$). The electron spins may be aligned with both moments parallel to the field $T_+(\alpha\alpha)$, with spin angular momentum $+\hbar$ along the field axis ($M_s = 1$); both antiparallel $T_-(\beta\beta)$ with spin angular momentum $-\hbar$ along the field axis ($M_s = -1$); or one spin parallel (α) and one spin antiparallel (β), T_0 ($\alpha\beta$) with zero spin angular momentum along the field axis ($M_s = 0$).
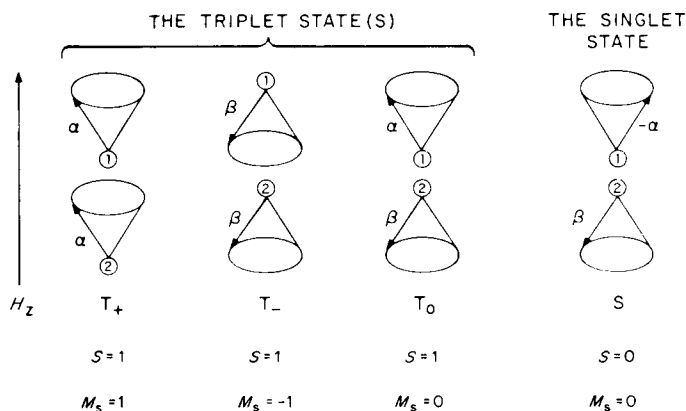

FIG. 2   Vector model of the singlet and triplet states of a radical pair

Thus, a transformation from S to T_0 requires a rephasing of the two spin vectors with respect to each other, whereas S to $T_\pm$ requires a spin flip, i.e. a change in total electronic spin momentum. Transitions between the triplet and singlet states (intersystem crossing) are forbidden in the absence of other magnetic interactions. However, in the next section, we shall discuss the magnetic interactions which cause the breakdown in the "forbiddenness" of such state-changing processes.

Importance of spin states in radical pair chemistry

If the two radicals which are produced from a singlet molecule should re-encounter, then a molecular product from radical combination or disproportionation may result. Such a product is described as resulting from a geminate recombination. A bond will be formed during the encounter only if the electron spins correspond to a singlet state. Encounters involving triplet state radical pairs are unproductive. Processes which transform initially

formed singlet radical pairs into triplet radical pairs prevent geminate re-encounters from forming products. When this occurs, escape of either radical from the initial solvent cage becomes more likely, and thus non-geminate, or random, encounters become more probable. Products which arise from geminate encounters are termed cage products; those from random encounters are escape products. Hence, an intersystem crossing process in an initially formed singlet radical pair will tend to increase the formation of escape products (and increase cage products for initially triplet radical pairs). Furthermore, if the intersystem crossing transformation is modulated by the magnetic field, then the origin of magnetic field effects on chemical reactions may be realized. The crucial condition for observation of magnetic field effects is a *competition* between two processes: one of the processes must be magnetic field dependent, the other is magnetic field independent[1]. For the example of radical pair chemistry, the processes are intersystem crossing (field dependent) and diffusive escape from the solvent cage or reaction to form a chemically modified radical pair (field independent).

IMPORTANT INTERACTIONS IN RADICAL SYSTEMS

The mechanisms of intersystem crossing depend intimately upon the magnetic interactions that occur in radical systems both from internal molecular and external fields. These interactions are described in this section.

Single radicals

The interactions which are characteristic of single radicals are those which are probed in electron spin resonance (esr) experiments (Carrington and McLaughlan, 1967). Interaction of an electron spin with an applied magnetic field results in an energy difference between the parallel (α) and antiparallel (β) spin states. The energy gap is defined as $\Delta E = g\beta H$ (Fig. 3), where β is the electron Bohr magneton, H is the applied field, and g is a proportionality constant related to the total angular momentum of the electron. Just as the spin motion of a charged electron results in a magnetic moment, the orbital motion of an electron results in a contribution to the overall electronic angular momentum. Coupling of spin and orbital angular momenta causes a change in the total angular momentum for a given electron. Thus electrons in different radicals, which possess different orbital angular momenta, will interact to varying extents with an external field. The g-value is the experimental measure of the extent of interaction and, in effect, is analogous to the familiar chemical shift measured in nmr spectroscopy. The value of g is 2.0023 for a "free" electron and ranges from 2.0000 to 2.003

---

[1] More generally, the two processes should have *different* magnetic field dependences.

for typical carbon-based organic free radicals. Such values are determined by irradiating the radical with microwave radiation and varying an external magnetic field until the spin state energy gap equals the microwave photon energy and resonance occurs.
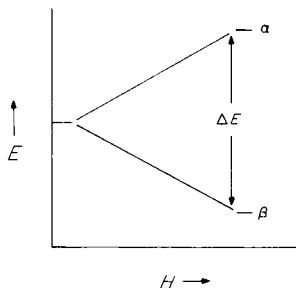

FIG. 3   Diagram showing the effect of an external magnetic field on the energy difference between the α and β spin states of a single electron

Additional intramolecular magnetic fields which may couple with the electronic magnetic moments arise from the spin moments of magnetic nuclei. These couplings lead to splittings in the absorption lines observed in esr spectra and are termed hyperfine couplings. Since the esr spectrum is recorded by varying the magnetic field, the splittings are observed at different values of the applied field, and the separation (called the hyperfine splitting constant, a) is usually expressed in gauss (G). The size of a particular hyperfine interaction is directly related to the electron density of the unpaired electron on the coupling nucleus. Typical values of a for protons range from 25 G to less than 1 G (c. 10^{-6} kcal mol^{-1}), but can reach 200 G for ^{13}C nuclei. Esr parameters for the organic radicals produced by homolytic cleavage of dibenzyl ketone are shown in Fig. 4.

Radical pairs

A non-magnetic electron exchange phenomenon occurs between interacting unpaired electrons. Interacting electrons are not allowed to be specifically defined as being located on one particular radical centre. In effect, the exchange processes, which are distinguished from Coulombic interactions by their dependence on spin, serve to preserve electron indistinguishability. As a result of these exchange interactions, the energies of the singlet and triplet states differ by $2 \times J$, where J is the electron exchange integral. The size of the exchange integral is determined in part by the separation of the two radical pair centres (Fig. 5). As the components of a radical pair begin to diffuse apart, the exchange interaction falls off rapidly. At a certain distance (c. 10 Å for typical organic radical pairs), J becomes negligible and the singlet and triplet states become energetically degenerate. At this point, intersystem crossing processes become energetically feasible.
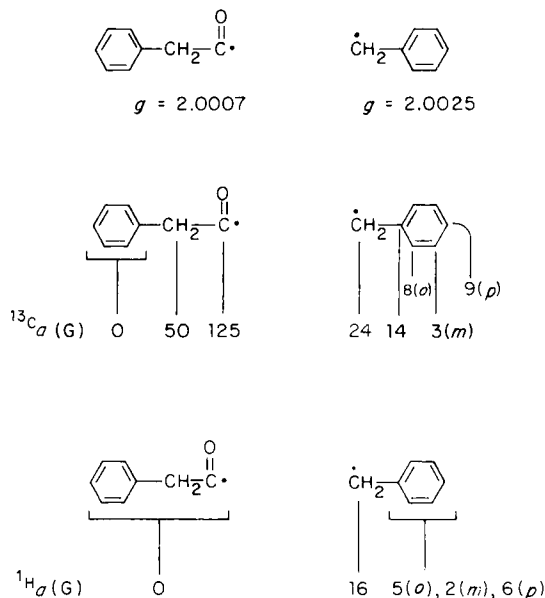
FIG. 4 Esr parameters of the $C_6H_5CH_2^{\cdot}$ and $C_6H_5CH_2CO\cdot$ radicals which are formed upon photolysis of dibenzyl ketone. (Hyperfine couplings, a, in gauss)
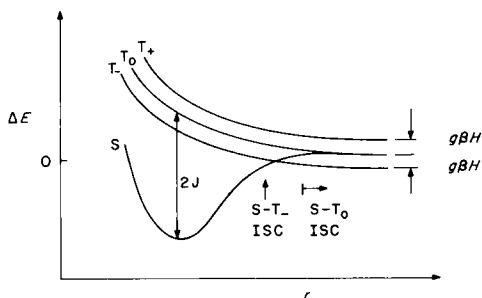
FIG. 5 Potential energy diagram showing the effect of separation of the partners in a radical pair (r), on the energy difference between the singlet and triplet states (ΔE). As r increases, the exchange integral (J) decreases. When J, and thus ΔE become negligible, intersystem crossing becomes energetically allowed. The application of a magnetic field causes a splitting in the energy levels of the T_+, T_0 and T_- states (Zeeman effect). The size of the splitting is given by $g\beta H$, where $g = (g_A + g_B)/2$

Finally, an important interaction in the context of the present discussion is that with an external magnetic field. As previously described, the application of a magnetic field to a radical pair system results in the alignment of the spin vectors for each electron along the axis of that field (Fig. 1). Because two of the triplet substates have non-zero projections of their spin momenta along the axis of the field, the three substates become non-degenerate. Those radical pairs with "up" or α electron spin, $M_s = 1$ (T_1), are raised in energy and those with β spin, $M_s = -1$ (T_-), are lowered in energy. The energies of the T_0 and S states remain unchanged. This splitting of the three sublevels upon application of an external magnetic field is commonly called the Zeeman effect. The extent of the splitting is given by the Zeeman energies which are $(g_A + g_B)\beta H/2$, 0, $-(g_A - g_B)\beta H/2$ for T_+, T_0 and T_-, respectively. The effect is shown diagrammatically in Fig. 5.

MECHANISMS OF INTERSYSTEM CROSSING

As mentioned previously, the theory of magnetic field effects on radical pair reactions comes directly from the theory of CIDNP, which considers two main mechanisms for intersystem crossing. These intersystem crossing processes, and the magnetic field effects upon them, arise as a direct consequence of the interactions described in the previous section.

As the two radical centres in a radical pair begin to separate, the exchange interaction (J) which both couples the precessional motion of the two electron spins, and maintains a difference in the energies of the S and T_0 states, becomes negligible relative to the interactions of the individual electrons with external fields, and with nearby magnetic nuclei (a). Instead of precessing strictly in phase, as when coupled by J, each electron spin now precesses at a different rate determined by the magnetic interaction to which it is coupled. Actually, J need not become zero for intersystem crossing to occur (*vide infra*); however, for the following discussion it will be assumed that J is zero, i.e. T_0 and S are degenerate.

An initially formed, singlet radical pair remains in a singlet state if the precessional frequencies remain the same for the two electrons, i.e. the difference in precessional rates ($\Delta\omega$) remains zero. This is the case if the magnetic fields experienced by the two electrons on the radical pair centres are the same. However, if these magnetic fields should differ, then the precessional rates may become unequal ($\Delta\omega \neq 0$), and the electrons will lose their singlet phasing. This implies acquisition of the triplet phasing, as shown diagrammatically in Fig. 6. In fact, because the precessional frequencies remain different, given sufficient time, the spin state will pass through pure triplet (T_0) and continue back to singlet (S). The radical pair spin state will be a sinusoidally varying mixture of singlet (S) and triplet (T_0) states.
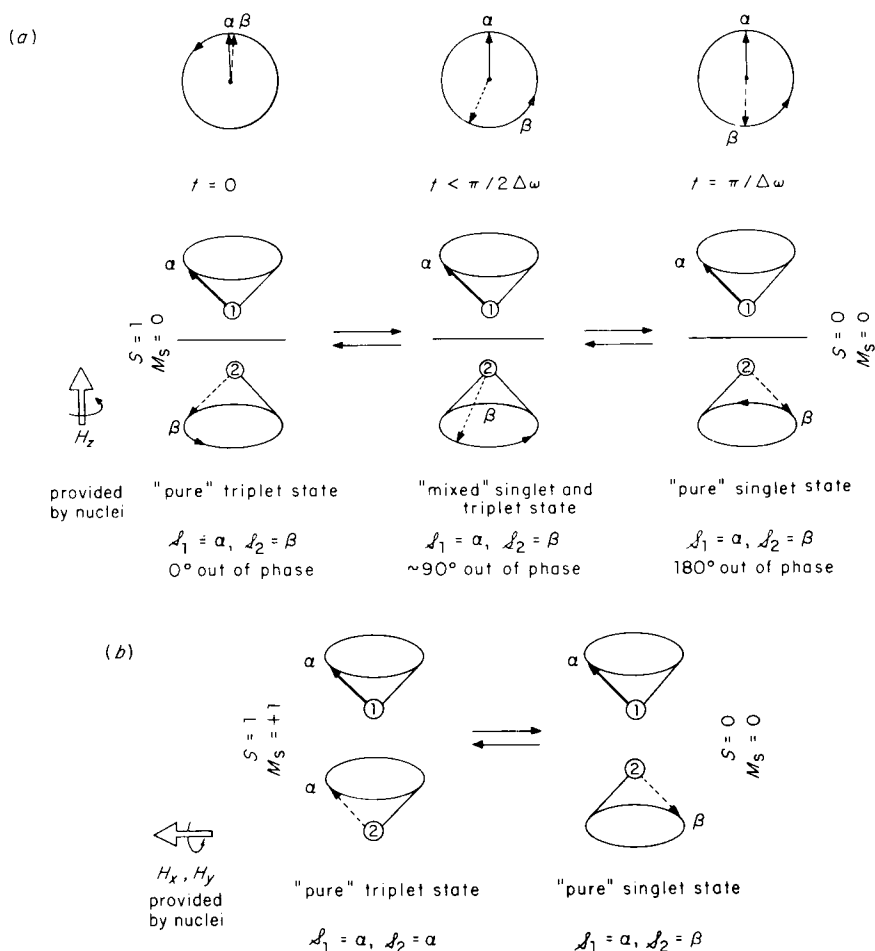
FIG. 6   (a) A spin clock and vectorial representation of the $T_0 \rightleftharpoons S$ intersystem crossing mechanism in radical pairs. (b) A vectorial representation of a $T_+ \rightleftharpoons S$ intersystem crossing showing the required change in electron spin

An alternative and useful illustration of the $S \rightleftharpoons T_0$ intersystem crossing can be made in terms of a "clock" representation (Kaptein, 1977). If the z-axis corresponds to the direction of the applied field, then the projection of the spins in the xy-plane produces a vector description of the T_0 and S states that resembles the hands of a clock. When electron exchange is large relative to other interactions, then the clock can read only 12 or 6, i.e. T_0 and S do not mix. When electron exchange is small, then rephasing of the two spin vectors can occur and the clock can read any arbitrary time (Fig. 6).

The time τ_{ST} it takes to convert S to T_0 is the time required to rephase the two vectors by π radians. If $\Delta\omega$ equals the differential precessional rate in radians s^{-1}, then $\tau_{ST} = \pi/\Delta\omega$. The rate constant for intersystem crossing (the inverse of τ_{ST}) is thus given by (2). Hence, the mechanism of intersystem crossing from S to T_0 depends on the methods by which $\Delta\omega$ is caused to change from zero.

$$k_{ST} = \Delta\omega/\pi \qquad (2)$$

Intersystem crossing from T_+ or T_- to S requires a change in the z-component of electronic spin angular momentum from $1\hbar$ or $-1\hbar$ to $0\hbar$, respectively.[2] As is evident from the previous discussion, and from Fig. 2, the rephase mechanism which is used for $T_0 \to S$ intersystem crossing is incapable of promoting a change in the z-component of angular momentum. Instead, a mechanism is required which can "flip" the spin of one of the electrons i.e. an exchange of electron spin angular momentum with another source of angular momentum is required. Although the vector model implies that both a spin flip and rephase are required, actually only the former is necessary. The mechanism whereby the electron spin angular momentum is allowed to change makes use of the hyperfine coupling phenomenon. Thus, an electronic spin may exchange momentum with a nuclear spin to which it is coupled by means of a "double flip" in which each spin state, nuclear and electronic, is changed and thus total angular momentum is conserved. The effect is shown diagramatically in Fig. 6 in which a T_+ state is transformed into an S state *via* a flip in one spin vector.

Hyperfine coupling mechanisms

The electron-nuclear hyperfine coupling promotes intersystem crossing by two independent mechanisms. The presence of local nuclear magnetic fields, as transmitted to the electron spin *via* the hyperfine coupling, provide the torque required to rephase the electron spin vectors and promote $T_0 \rightleftharpoons S$ intersystem crossing (for radical pairs and other systems with $J \to 0$). In Fig. 6 it is shown how this torque, oriented around the z-axis, enables the rephasing of a T_0 to an S state to occur. The rate of intersystem crossing in terms of the $\Delta\omega$ factor is given in (3), where a_n is the hyperfine constant,

$$\Delta\omega \sim |\underset{i}{\Sigma} a_{1i} m_{1i} - \underset{j}{\Sigma} a_{2j} m_{2j}| \qquad (3)$$

and m_{ni} the spin states ($\pm 1/2$ for ^{13}C and ^1H) of nucleus i on radical n.

---

[2] Strictly this represents an oversimplification since at zero field a dynamic equilibrium exists between the three triplet substates and in effect only one mixed triplet state exists (see Kaptein, 1977).

For a radical pair consisting of identical radicals $(a_1 = a_2)^3$, $\Delta\omega$ can be non-zero provided the nuclear spin states on the two radicals differ.[4] For non-identical radical pairs $(a_1 \neq a_2)$, $\Delta\omega$ will be non-zero independent of the nuclear spin states, although some combinations of nuclear spin states will be more effective than others in promoting $T_0 \rightleftharpoons S$ intersystem crossing.

The hyperfine coupling also promotes $T_{\pm} \rightleftharpoons S$ intersystem crossing. In this case the local nuclear magnetic fields which act in the x- and y-axes can provide the torque necessary to flip the direction of an electron spin vector (Fig. 6). The hyperfine interaction causes transitions between radical electron-nuclear spin states which have the same total angular momentum and have similar energies. For example, an electron-nuclear spin system in the spin state $\alpha_e\beta_N$ will be transformed into the spin state $\beta_e\alpha_N$ (Fig. 7).
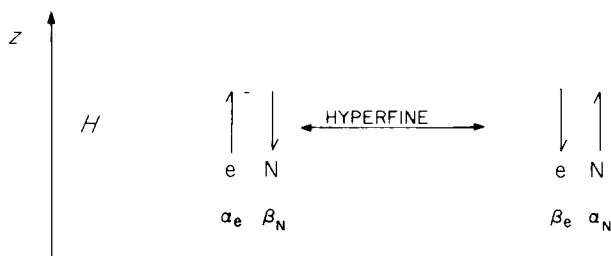

FIG. 7   Schematic representation of the mechanism by which hyperfine coupling causes a change in the z-component of the angular momentum of an electron (e). The simultaneous change in direction for both the electron and nuclear (N) spin vectors preserves the overall momentum in the system

In the triplet radical pair $[\alpha_{e1}, \alpha_{e2}\,\beta_N]$, T_+, this hyperfine transition produces the radical pair $[\alpha_{e1}, \beta_{e2}\,\alpha_N]$, S, a singlet radical pair. Hence, at zero applied magnetic field, hyperfine mechanisms exist which can induce intersystem crossing from each of the triplet levels to and from the singlet level (assuming $J = 0$). Application of a magnetic field causes splitting of T_+ and T_- from S due to the Zeeman effect, and destroys the degeneracy needed for the coupled nuclear-electronic spin flips. At applied fields about one order of magnitude greater than the hyperfine coupling, the processes of $T_+ \rightleftharpoons S$ intersystem crossing are shut off. Since the magnitude of hyperfine couplings are less than 100 G, at applied fields of >1000 G only radical pairs in the T_0 state can intersystem cross to S (by the rephasing mechanism).

[3]For simplicity, we consider the case of each electron being coupled to only one nucleus.
[4]Herein lies the basis for the observation of CIDNP effects (Kaptein, 1977) and of the unusually large, magnetically induced, ratio of reaction of ^{12}C vs ^{13}C in radical pairs compared to the ratio expected from mass isotope effects (see p. 33).

In terms of radical pair chemistry this means that the extent of cage reaction from a *singlet* radical pair will *increase* at fields > 1000 G relative to the zero field situation, because intersystem crossing is slowed down. In turn, the extent of cage reaction of a *triplet* radical pair will *decrease* at fields > 1000 G relative to the zero field situation.

In certain systems, such as radical pairs constrained to remain as proximate collision pairs and short chain diradicals, the electronic exchange interactions are of the order of 10^5G, so that even at zero applied field, the singlet and triplet states of the radical pair (or diradical) are not degenerate. In such circumstances, intersystem crossing cannot be effectively induced by hyperfine interactions. However, application of an external field of sufficient strength that the Zeeman splitting ($g\beta H$) matches the singlet-triplet splitting due to exchange ($2J$), will create a degeneracy between T_- and S (for singlet ground state radical pairs) (Fig. 5) and T_+ and S (for triplet ground state radical pairs). Thus, under these conditions, hyperfine induced spin-flip mechanisms become feasible because of the magnetic field imposed level crossing, i. e. at fields substantially lower or higher than that field required to cause a degeneracy of singlet and triplet states, intersystem crossing is inhibited. Numerous examples of these magnetic effects are known in diradical CIDNP research. In terms of diradical chemistry, a triplet diradical which can be scavenged intermolecularly would be expected to yield more "cage" or intramolecular products (due to coupling or disproportionation) at fields which induce level crossing.

The rate of hyperfine induced intersystem crossing (k_{ISC}) by the rephasing mechanism is given approximately by (4), where a is in G (Buchachenko,

$$k_{ISC} \sim 3 \times 10^6 a \qquad (4)$$

1976). Since typical values of a (for a single nucleus) fall in the range 10–100 G, $k_{ISC} \sim 3 \times 10^7$ to $3 \times 10^8 s^{-1}$. Comparable rates are expected for the spin-flip mechanism ($T_\pm \rightleftharpoons S$) in cases where the triplet-singlet gap is small compared to hyperfine interactions.

The Δg mechanism

If the individual components of a radical pair possess different g-factors ($\Delta g \neq 0$), a hyperfine independent mechanism (the "Δg" mechanism) for inducing intersystem crossing occurs. This mechanism operates only to induce $S \rightleftharpoons T_0$ intersystem crossing, and results from the relationships between the g-factor, the applied field, and the rate of spin-vector precession about an applied field. The rate of precession (ω) of a spin vector about a field direction is proportional to the g-factor and the strength of the field to which the vector is coupled as in (5).

$$\omega \sim g\beta H \qquad (5)$$

The difference in precessional rate ($\Delta\omega$) for the spin vectors of a radical pair is proportional to the difference of g-factors if the field is applied homogeneously across both radicals (6).

$$\Delta\omega \sim (g_1 - g_2)\beta H = \Delta g \beta H \tag{6}$$

An order of magnitude estimate for the rate constant for intersystem crossing is given by (7), where H is in gauss, and k_{ISC} is in s^{-1}. For typical

$$k_{\text{ISC}} \sim 3 \times 10^6 \Delta g H \tag{7}$$

carbon-centred organic radicals, Δg varies from 0.5×10^{-3} to 5×10^{-3}. Thus, in the earth's field (~ 1 G), maximal values of k_{ISC} for carbon-centred radical pairs fall in the range of 10^3–10^4s^{-1}. In strong laboratory magnetic fields ($\sim 10^5$G), the values of k_{ISC} for carbon-centred radical pairs fall in the range 10^8–10^9s^{-1}. In the upper range, the value of k_{ISC} is comparable to or greater than that for hyperfine-induced $T_0 \rightleftharpoons S$ intersystem crossing.

In summary, both a- and Δg-mechanisms can contribute to $T_0 \rightleftharpoons S$ intersystem crossing of carbon-centred radical pairs. A more general relationship for k_{ISC}, for the case of $T_0 \rightleftharpoons S$ intersystem crossing, is therefore given by (8). The contributions of Δg and a to k_{ISC} can be constructive or destruc-

$$k_{\text{ISC}} \sim 3 \times 10^6 [\Delta g H + \sum_i a_{1i} M_{1i} - \sum_j a_{2j} M_{2j}] \tag{8}$$

tive depending upon the relative signs of the pertinent constants and spin states.

The golden rule

The previous discussion describes the mechanisms of intersystem crossing using a convenient and easily understandable model, the vector spin description. A more complete description of the intersystem crossing process arises from the postulates of quantum dynamics. A "golden rule" expression (9) is available for understanding the rates of transitions between states of differing energies (non-degenerate) in terms of quantum dynamics, where ME represents the matrix element coupling the two states, and ΔE their

$$k_{\text{ST}} \approx \frac{1}{\hbar} \frac{<\text{ME}>^2}{\Delta E} \tag{9}$$

energy gap (Atkins, 1970). The matrix elements for the transitions for each triplet substate are given in (10), (11) and (12) (Buchachenko, 1976) where I_i is the spin quantum number of nucleus i, and M_i is the projection of the

spin along the magnetic field direction. For the case of interactions with a

$$< T_0|\mathscr{H}|S> \ = 1/2\Delta gH + a_i m_i - a_j m_j \tag{10}$$

$$< T_+|\mathscr{H}|S> \ = -(1/8)^{1/2} a_i[I_i(I_i + 1) - m_i (m_i - 1)] \tag{11}$$

$$< T_-|\mathscr{H}|S> \ = (1/8)^{1/2} a_i[I_i(I_i + 1) - m_i (m_i + 1)] \tag{12}$$

single magnetic nucleus of spin 1/2, e.g. ^1H or ^{13}C, $I_i = 1/2$, (11) and (12) reduce to (13) and (14). The matrix elements reveal the different behaviour of the triplet substrates at low field. Equation (9) shows that as the energy gap

$$< T_+\beta|\mathscr{H}|S\alpha> \ = -(1/8)^{1/2} a_i \qquad < T_+\alpha|\mathscr{H}|S\alpha> \ = 0 \tag{13}$$

$$< T_-\alpha|\mathscr{H}|S\alpha> \ = 0 \qquad < T_-\alpha|\mathscr{H}|S\beta> \ = -(1/8)^{1/2} a_i \tag{14}$$

between the states increases, the transition rate between the states decreases toward a limiting value of zero.

Environmental effects

Many magnetic field effects on the chemistry of radical pairs have their origin in the competition between intersystem crossing and escape from the solvent cage. If escape is very fast relative to intersystem crossing and is also irreversible, then the number of radical pairs undergoing intersystem crossing will be small. In this case, magnetic field effects on the reactions of the pair will also be small. If an environment can be produced which allows diffusive separation such that J is allowed to diminish to such an extent as to allow intersystem crossing, but which slows irreversible diffusive separation, then the competition between intersystem crossing and diffusion may be controlled so that the effect of an external magnetic field may be increased. Evidently, the observation of significant magnetic field effects requires a proper balance of the rates for diffusion, intersystem crossing, and electron exchange inter-actions. Certain examples in the next section illustrate the usefulness of changing solvent viscosity and of utilizing microheterogeneous environments such as micelles to influence the diffusion term, so that magnetic field effects may be magnified.

CLASSIFICATION OF MAGNETIC FIELD EFFECTS

An overview of the literature allows division of the magnetic field effects into four classes. Of these, three are observed upon the application of an external laboratory magnetic field and can be distinguished in terms of the intersystem crossing mechanisms discussed previously. The fourth class of effect is attributable entirely to the local magnetic fields which are character-istic of magnetic nuclei.

Class I effects

Class I effects are defined as those in which $J \approx 0$ and for which intersystem crossing occurs predominantly by the hyperfine mechanisms. The effects are characterized by a decrease in intersystem crossing as a function of field (Fig. 8), a result of the Zeeman splitting of the triplet sublevels. Since the T_+ and T_- states become non-degenerate with the S state, $T_\pm \rightleftharpoons S$ intersystem crossing is prevented and thus the overall rate of intersystem crossing is slowed down. The maximum effect is observed when the external field exceeds the magnitude of the hyperfine couplings. In Fig. 8 this field is shown as H_I and is typically *c.* 1000 G.
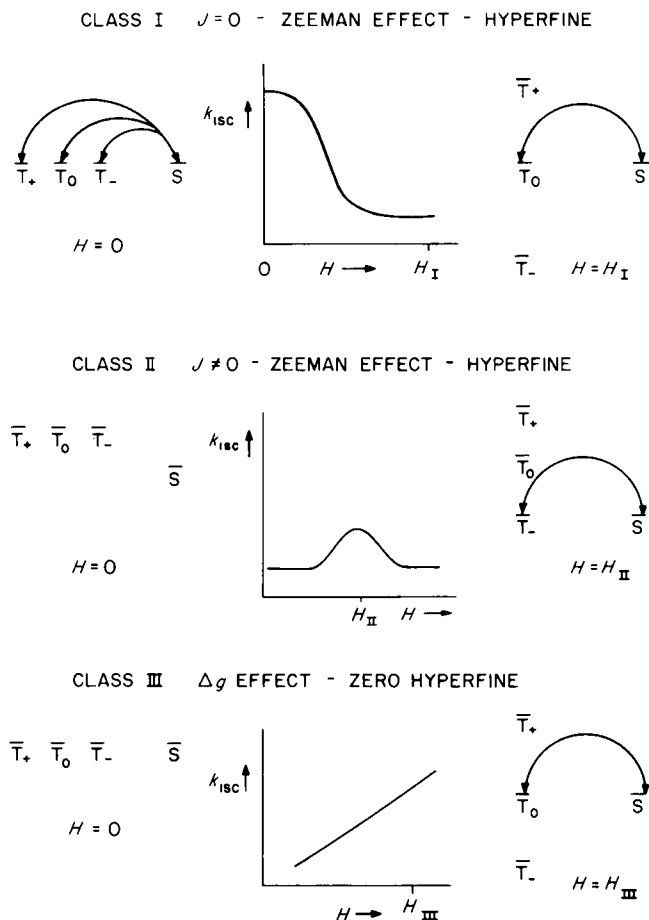

FIG. 8   Diagram showing the three types of behaviour of k_{ISC} as a function of applied field which allows classification of the external magnetic field effects

Class II effects

Class II effects are defined as those in which $J \neq 0$ and for which intersystem crossing is hyperfine induced. These effects are characterized by an increase in intersystem crossing around an external field strength at which the Zeeman splitting is approximately equal to J (H_{II} in Fig. 8). At this field the Zeeman splitting of the triplet sublevels causes a degeneracy between one triplet state and the singlet state. Intersystem crossing can thus occur at this external field strength. Above or below this value of the applied field, the appropriate degeneracy does not exist, and thus intersystem crossing is inefficient.

Class III effects

Class III effects are observed for reactions in which the Δg-mechanism is responsible for intersystem crossing. These effects are characterized by an increase in intersystem crossing rate as a function of applied field, since the rate of precession of an electron spin vector about an applied field is directly proportional to the strength of that field. These effects are commonly only observed at very high external magnetic fields (i.e. H_{III} in Fig. 8 > 10^5G).

Class IV effects

Class IV effects are those for which $J \approx 0$, $\Delta gH \approx 0$, and $a \neq 0$. This class differs from the previous three because the magnetic field which dominates the effect is due to the magnetic moments of nuclei; hence, class IV effects are termed *magnetic isotope effects*. These effects allow a differentiation in the behaviour of radical pairs containing magnetic nuclei from radical pairs containing nonmagnetic nuclei or, more generally, allows a differentiation in the behaviour of radical pairs possessing nuclei of differing magnetic moments.

2 Experimental examples

CLASS I EFFECTS: REACTIONS INFLUENCED BY THE ZEEMAN EFFECT

Experimental examples of class I effects are the most common and best documented of all known magnetic field effects on organic chemical reactions. They involve both initially singlet and triplet radical pairs.

One of the first magnetic field effects was reported by Sagdeev *et al.* (1973a,b) who noted a substantial magnetic field effect on the product ratio from the reaction of n-butyllithium with benzyl chloride and with penta-fluorobenzyl chloride ($C_6F_5CH_2Cl$). The reaction is summarized in Scheme 1 (Molin *et al.*, 1979). n-Butyllithium was decomposed in the presence of penta-fluorobenzyl chloride in boiling hexane. The reaction was performed both in the earth's field (~ 1 G) and at 18 kG. The reaction products were analysed

$$ArCH_2Cl \ + \ C_4H_9Li \ \longrightarrow \ ArCH_2CH_2Ar \ + \ ArCH_2C_4H_9 \ + \ C_4H_9C_4H_9$$

$$\Big\downarrow -LiCl \qquad\qquad\qquad\qquad AA \qquad\qquad\quad AB \qquad\qquad BB$$

$$ArCH_2^{\cdot} \ + \ \cdot C_4H_9$$
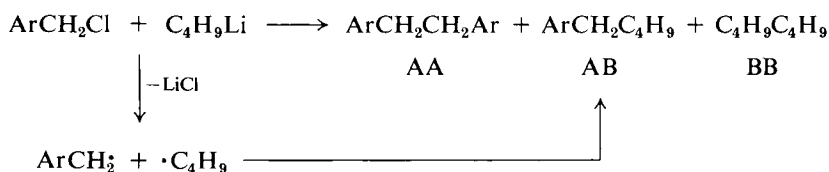
Scheme 1

by ^{19}F nmr spectroscopy. It was found that the amount of the product AB (Scheme 1) relative to product AA, increased by 30% when the reaction was performed in the presence of the applied field. Similarly, an increase in this ratio of 20% was found for the reaction of n-butyllithium and benzyl chloride in the presence of a 25 kG field. Subsequently, more detailed studies (Molin et al., 1979) revealed that the effect was apparent at very low fields and that the ratio reached a constant value above an applied field of about 200 G. It is postulated that both reactions involve the formation of a singlet geminate radical pair (A $\cdot \cdot$ B, benzyl $\cdot \cdot$ butyl) in a primary solvent cage. A competition then is created between cage reaction (recombination to form product AB) and diffusive separation to give free radicals. However, inter-system crossing within the solvent cage, to produce a triplet radical pair, will result in less efficient cage reaction and hence less efficient formation of AB. It is assumed that the free radicals A and B will produce AA, AB and BB in statistical yields (25%, 50%, and 25%, respectively). The application of a magnetic field inhibits the occurrence of S $\rightarrow$ T$_{\pm}$ intersystem crossing. Hence the radical pair retains its singlet character longer and thus more efficient cage reaction results. The observation of the field effects in as weak a field as 200 G is consistent with the Zeeman mechanism as the origin of the magnetic field effect. Since the origin of the magnetic field effect lies in the competition between intersystem crossing and diffusive separation, a change in magnetic field effect should be observed if the rate of diffusion is changed and if the rate of intersystem crossing is held constant. Sagdeev tested this prediction by performing experiments in solvents of differing viscosity. It was found that an increase in the magnetic field effect of 15% could be obtained by increasing the solvent viscosity by 0.6 cP.

The work of Turro et al. (Turro, 1981, 1983; Turro and Kraeutler, 1980) on the photochemistry of aromatic ketones provides many examples of class I magnetic field effects. Photolysis of dibenzyl ketone (DBK) and substituted DBK's has been shown to proceed by the mechanism outlined in Scheme 2 (Engel, 1970). Photolysis initially yields a phenacyl radical and a benzyl radical and leads, after decarbonylation, to two benzyl radicals. Thus, potentially, these systems can exhibit magnetic effects from two radical pairs. Photolysis of an unsymmetrical DBK can lead to the formation of three diphenylethane

$$ArCH_2COCH_2Ar \xrightarrow{h\nu} S_1 \longrightarrow T_1 \longrightarrow ArCH_2CO\cdot + \cdot CH_2Ar$$

Primary radicals

$$ArCH_2CH_2Ar \longleftarrow ArCH_2^\bullet + ArCH_2^\bullet + CO$$

Secondary radicals
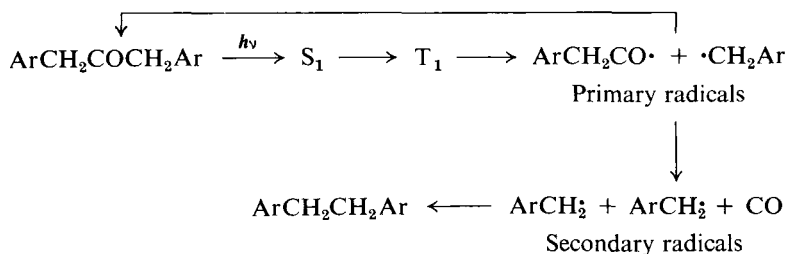
Scheme 2

(DPE) products according to (15). The ratio of the products AA : AB : BB

$$PhCH_2COCH_2Ar \rightarrow \underset{AA}{PhCH_2CH_2Ph} + \underset{AB}{PhCH_2CH_2Ar} + \underset{BB}{ArCH_2CH_2Ar} \qquad (15)$$

will be 25 : 50 : 25 if there is no cage effect, and 0 : 100 : 0 if cage recombination is 100% efficient. A numerical value for the cage effect for intermediate situations is defined by (16). Experimentally, it is found that the cage effect in homogeneous solution is 0% for photolysis of p-xylyl benzyl ketone

$$\% \text{ cage products} = \frac{AB - (AA + BB)}{AA + AB + BB} \times 100 \qquad (16)$$

(Turro and Cherry, 1978). In this case, because the initial radical pair is in a triplet state (Scheme 2), the formation of cage products requires an inter-system crossing which cannot compete with diffusive separation. Hence a cage effect of zero is observed. Evidently, the observation of cage effects, and thus magnetic field effects, for initially triplet radical pairs requires an environment which allows intersystem crossing to compete with diffusive separation. Certain solution phase systems possess a micro-heterogeneous environment which may severely restrict the diffusional mobility of an organic solute. Specifically, aqueous solutions of ionic detergents, which commonly have a hydrophobic hydrocarbon "tail" and a hydrophilic ionic "head", aggregate above a certain concentration (critical micelle concentration, cmc) to form micelles (Fendler and Fendler, 1975). In Fig. 9 is shown a schematic model of a micelle. Micelles of the most commonly used detergents typically have maximal cross-sections of 20–30 Å, which correspond to ~50–100 detergent molecules. The hydrophobic core provides a volume of hydrophobic space (in an otherwise aqueous environment) that is capable of solubilizing an organic substrate. In effect, micelles can provide a cage environment for organic molecules. A geminate radical pair which is generated by homolytic cleavage of a molecule which is solubilized in a

micelle will remain geminate until one or both radicals escape into the bulk aqueous phase. For non-viscous organic solvents at ambient temperature, the residence time of a primary geminate pair in a solvent cage is $\sim 10^{-10}$ to 10^{-11}s.

Aqueous bulk phase

⊘ WATER MOLECULE

∿∿● DETERGENT MOLECULE

TYPICAL IONIC DETERGENTS

$CH_3(CH_2)_{11}SO_4^{\ominus} \; Na^{\oplus}$ SDS

$CH_3(CH_2)_{15}N^{\oplus}(CH)_3 \; Cl^{\ominus}$ HDTCl

Range of shear surface

Core

20 - 30 Å

Stern layer up to a few Å

Gouy - Chapman layer up to several hundred Å

outside

inside

boundary
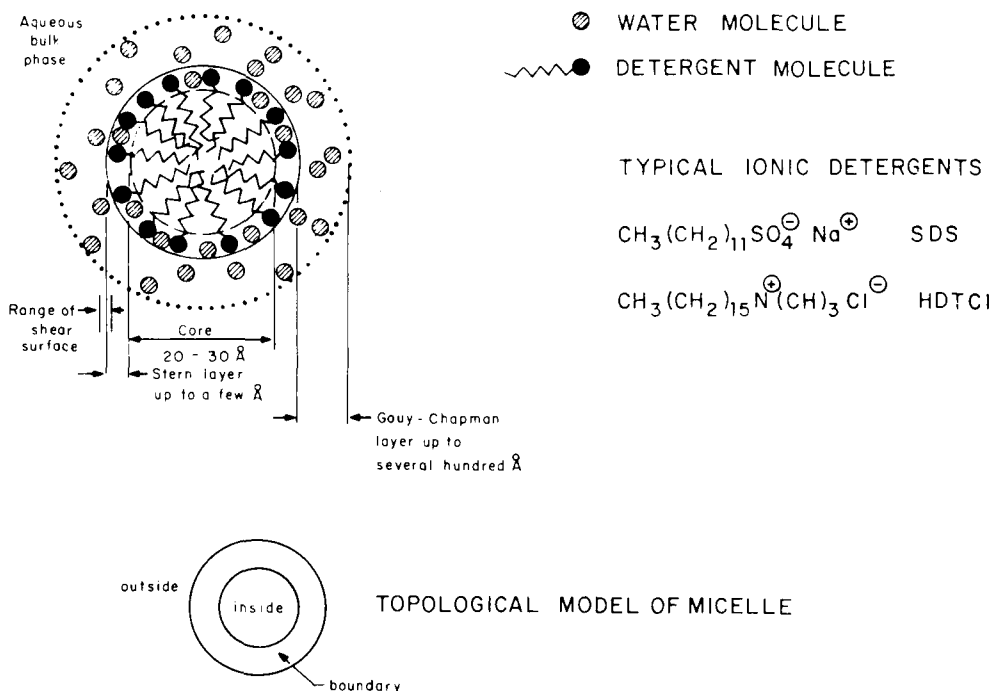
TOPOLOGICAL MODEL OF MICELLE

FIG. 9   Schematic model of micelle aggregates formed by addition of hexadecyltrimethylammonium chloride (HDTCl) or sodium dodecylsulphate (SDS) to water

In contrast, for radicals possessing six or more carbons, the residence time of a pair in a micelle cage is $> 10^{-6}$s. Additionally, the "volume" of a solvent cage is roughly the size of the solvated radical pair, whereas the volume of the micelle cage is such that the component radicals of a pair are allowed to separate by distances up to tens of Å. Thus, micellar systems can potentially allow an initially triplet geminate radical pair to separate so that J becomes negligible, but provide a reflecting boundary, at the Stern layer (Fig. 10), to the geminate character of the pair to allow intersystem crossing to compete with diffusive separation. (For reviews on the effects of micelles on reactions of radical pairs, see Turro et al., 1980b; Turro, 1981, 1983.) Experimentally, it is found that photolysis of p-xylyl benzyl ketone in HDTCl micellar solution yields a non-statistical distribution of diphenylethanes. In this case, using (16), a cage value of $\sim 30\%$ may be computed (Turro et al., 1980a).
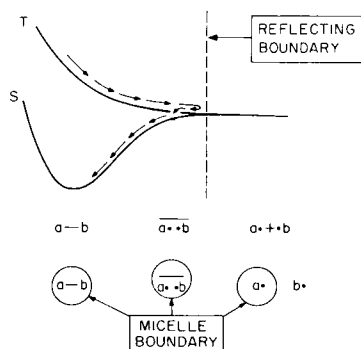
FIG. 10   Diagram showing the effect of a micelle in maintaining the lifetime of an initially triplet radical pair so as to allow more efficient intersystem crossing

Evidently, the micelle environment allows the initially triplet benzyl p-xylyl radical pair to develop sufficient singlet character to allow cage reaction to compete with irreversible diffusive separation. The use of micelles allows an alternative measure of cage reaction which may be used to probe the reactivity of symmetrical ketones. Addition of a sufficiently high concentration of a water soluble selective radical scavenger (e.g. cupric ions) allows the determination of the fraction of cage reaction according to (17), where $[AB]_{US}$ represents the amount of unscavengable coupling product, and $[ACOB]_R$ is

$$\text{Cage} = \frac{[AB]_{US}}{[ACOB]_R} \qquad (17)$$

the amount of reacted ketone (Turro *et al.*, 1980a). Only radicals which give coupling products within the micelle cage are not scavenged, and thus the amount of cage reaction is determined directly. Both methods of cage determination have been shown to yield experimentally identical results.

Upon application of an external magnetic field, a change in the % cage products is observed. A plot of the percentage of cage reaction for the micellar photolysis of DBK *vs* magnetic field is reproduced in Fig. 11. It can be seen that the cage effect drops quickly from 30% at zero G to 20% as fields of a few hundred gauss are imposed upon the sample, and then remains constant from 500 G to 5000 G. It has been proposed that the magnetic field effect on the percentage of cage reaction reflects the behaviour of the secondary (benzyl benzyl) radical pair. The quantum yield for disappearance of DBK (which is equivalent to the quantum yield for DPE production) in homogeneous organic solvent is ~ 0.7; however, this value drops to ~ 0.3 in

HDTCl micellar solution (Turro *et al.*, 1979b). This decrease must be attributable in part to a more efficient recombination of the primary (benzyl phenacyl) radical pair. In effect, the cage reaction for the primary pair is increased as a result of micellization for the same reason as for the secondary pair, i.e. the radical pair lifetime is increased so that intersystem crossing can compete with the process removing the radical pair. One important difference for the case of this radical pair is that the step which removes the radical pair is loss of carbon monoxide within the micelle, and not exit of one partner from the micellar cage environment. However, this step is magnetic field independent and thus the requisite competition for magnetic field exists. As expected, it is found that the quantum yield for DPE production is magnetic field dependent; the results are illustrated in Fig. 11
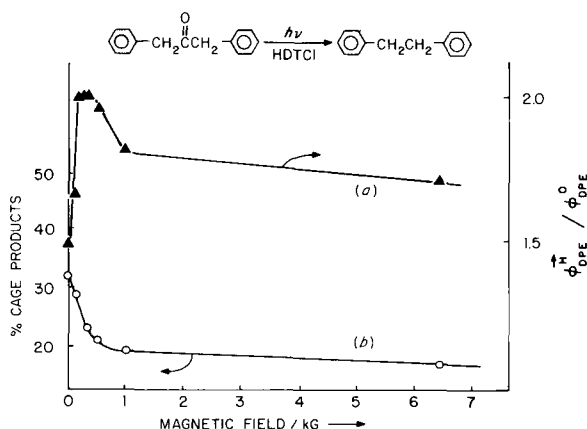
FIG. 11 Plot showing the effect of an external magnetic field of (*a*) the quantum yield for reaction relative to a standard ketone, and (*b*) the cage value for DPE production for photolysis of dibenzyl ketone in HDTCl micelles

(Chung, 1982), where the quantum yield relative to a standard DBK at 0 G. is plotted as a function of field. Remarkably for this radical pair an initial increase in relative quantum yield to a maximum at ~ 200 G is observed, followed by a decrease to an overall higher value. These effects on the two radical pairs are explicable by reference to Fig. 12. For the case of the secondary radical pair (^{3}RP', Fig. 12), the competition between k_{ex} and k_{TS}' determines the cage value. Since k_{ex} is independent of magnetic field and k_{TS}' is slowed by an external field due to Zeeman splitting of $T_{\pm}$, a lower cage effect results. For the case of the primary radical pair (^{3}RP, Fig. 12), the competition is between k_{-CO} and k_{TS}. Thus, as k_{TS}' is slowed by the external field, recombination to generate the starting material becomes less efficient

FIG. 12   Reaction scheme for discussion of magnetic field effects on the photochemistry of DBK in micellar solution. The encircled species represent micellized molecules or radicals

and thus, the quantum yield for reaction increases. A magnetic field dependence of the quantum yield for formation of a minor product (PMAP in Fig. 12), an isomer of DBK, is also observed.

An alternative probe for the reactions of the primary radical pairs formed from the photolysis of dibenzyl ketones is 2,4-diphenylpentanone (DPP) (Baretz and Turro, 1983). Irradiation of stereochemically pure ($\pm$) or *meso*-DPP in pentane leads to the products shown in (18) but no observable isomerization in the starting ketone. Irradiation of stereochemically pure DPP

in HDTCl micelles results in a different product distribution. In this case the products are isomerized starting ketone (8%), 3% phenylpropionaldehyde [4] is formed, and diphenylbutane [3] formation is reduced to 72%. Thus, the micellar medium again provides the environmental constraint necessary for cage reaction. Photolysis of DPP in micellar media also results in a decrease in quantum yield for reaction of DPP (0.62, 0.50, and 0.33 in pentane, HDTCl and SDS micelles, respectively). Application of an external magnetic field results in a decrease in the isomerization yield for systems in which cage reaction is significant. Isomerization efficiency is determined from plots of

% isomerization *vs* % conversion. The slopes of such plots for DPP under various reaction conditions are reproduced in Table 1. Evidently, in the presence of a 3 kG magnetic field, intersystem crossing in the primary pair is reduced so that the isomerization efficiency is lowered. Interestingly, it has

TABLE 1

Isomerization efficiencies as a function of magnetic field for photolysis of 2,4-diphenylpentanone[a]

Environment	Field/kG	Efficiency	Φr
Pentane	0	0.00	0.62
SDS	0	0.15	0.33
SDS	3	0.10	—
HDTCl	0	0.11	0.50
HDTCl	3	0.07	—
Porous glass	0	0.17	—
Porous glass	3	0.12	—

[a]Baretz and Turro, 1983

been shown that micelles are not a unique environment for the observation of these effects. For example, photolysis of DPP in porous glass reveals both cage and magnetic field effects (Baretz and Turro, 1983).

Photolysis of 1,3-diphenylbutan-2-one (DPB) yields, after decarbonylation, three coupling products (AA, AB, BB) which are a direct measure of the extent of cage reaction in the secondary radical pair (19) (Baretz and Turro, 1983). Analysis of the cage effect in a variety of "supercage" environments enables determination of magnetic field effects as a function of these environments (Table 2). The magnetic effects are attributable to the competition
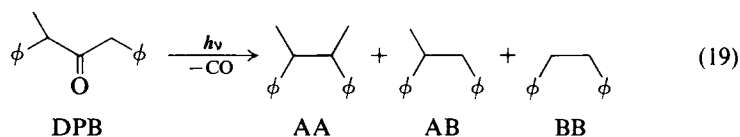
between intersystem crossing and diffusive separation of the radical pairs in the different environments. Large magnetic effects on the secondary radical pair reactions are possible in certain environments (for example, in porous glass, the magnetic effect was 61%).

Another example for which triplet radical pair reactivity may be modified by the use of micellar environments and a magnetic field is provided by the photolysis of 1,2-diphenyl-2-methylpropanone (DPMP) (Turro and Mattay, 1981). In homogeneous solution the main products are styrene and dicumyl; benzil and benzaldehyde are minor products (Scheme 3). In HDTCl solution

TABLE 2

Magnetic field effects on cage reactions of benzyl: sec-phenethyl radical pairs in micelles and on silicate surfaces[a]
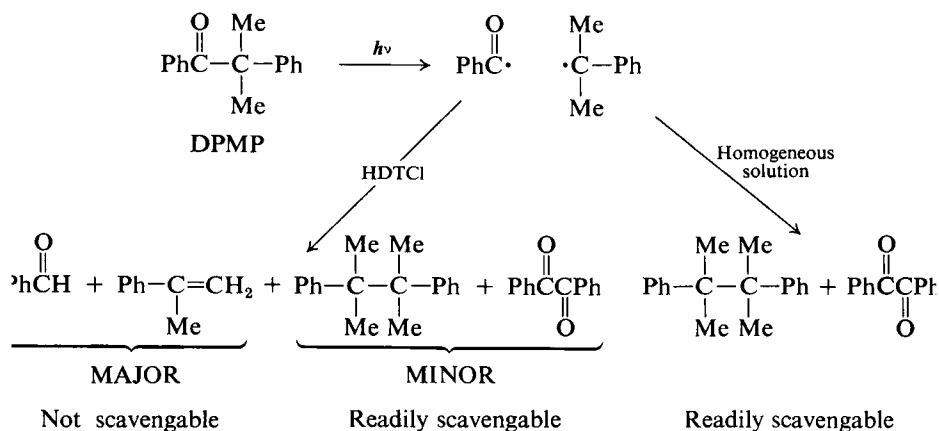
| Environment | % cage products[b] | | Magnetic field effect (%) |
	0 kG	3 kG	
HDTCl	71	52	−27
SDS	74	50	−32
Porous glass	38	15	−61
TLC[c]	9	6	−32
RPTLC[d]	15	11	−26

[a] Baretz and Turro, 1983
[b] Error limits ± 10%
[c] Photolysis performed on a silica TLC plate in an evacuated cell
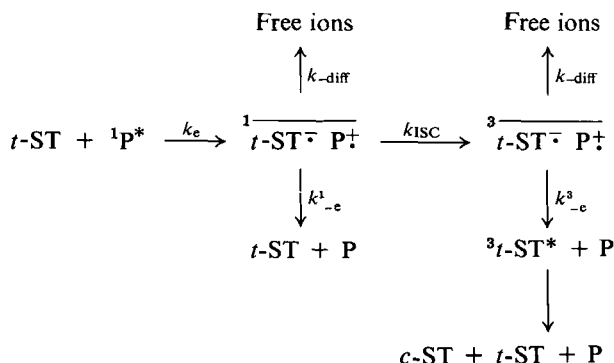[d] Photolysis performed on a reverse phase TLC plate in an evacuated cell

Scheme 3

the major products are styrene and benzaldehyde. As in the case of DBK, the cage effect for photolysis can be evaluated from Cu(II) quenching experiments. In fact, the addition of Cu(II) does not affect the production of styrene and benzaldehyde, and thus the yield of these disproportionation compounds gives the cage effect. The yield of cage products drops from 30% to a value of 20% in a field of 1000 gauss. In this case the initially triplet (benzoyl cumyl) radical pair may undergo intersystem crossing to yield the disproportionation products benzaldehyde and styrene, or escape to yield the coupling products dicumyl and benzil. In the presence of a magnetic field, intersystem crossing from $T_{\pm}$ is inhibited, and hence the cage effect is lowered.

Sagdeev (Leshina *et al.*, 1980) has reported that the pyrene sensitized *trans-cis* isomerization of stilbene is magnetic field dependent. Irradiation of pyrene in homogeneous solution in the presence of *trans*-stilbene leads to isomerization of the stilbene. The amount of isomerization, measured by nmr methods, was found to decrease by 30% when the reaction was performed in magnetic fields of greater than 100 G. The effect may be explained by reference to Scheme 4. Electron transfer (k_e) from the excited state of

$$
\begin{array}{ccc}
\text{Free ions} & & \text{Free ions} \\
\uparrow {\scriptstyle k_{-\text{diff}}} & & \uparrow {\scriptstyle k_{-\text{diff}}} \\
t\text{-ST} + {}^1\text{P}^* \xrightarrow{k_e} {}^1\overline{t\text{-ST}^{\bar{\cdot}}\ \text{P}_{\cdot}^{+}} \xrightarrow{k_{\text{ISC}}} {}^3\overline{t\text{-ST}^{\bar{\cdot}}\ \text{P}_{\cdot}^{+}} \\
\downarrow {\scriptstyle k^1_{-e}} & & \downarrow {\scriptstyle k^3_{-e}} \\
t\text{-ST} + \text{P} & & {}^3t\text{-ST}^* + \text{P} \\
& & \downarrow \\
& c\text{-ST} + t\text{-ST} + \text{P} &
\end{array}
$$

Scheme 4

pyrene (P) to *trans*-stilbene (*t*-ST) leads to a singlet radical ion pair. This ion pair may transfer the electron back to form the starting materials (k'_{-e}), undergo diffusive separation ($k_{-\text{diff}}$), or undergo intersystem crossing within the solvent cage to form a triplet radical ion pair (k_{ISC}). Back electron transfer within this species leads to the triplet state of stilbene which is the active *trans-cis* isomerization intermediate (Turro, 1978b). Application of a magnetic field will slow down the rate of intersystem crossing within the radical ion pair leading to a decrease in production of triplet-stilbene and hence of isomerization.

One of the first examples of a magnetic field effect on a chemical reaction was reported by Gupta and Hammond (1972). It was found that for photosensitized isomerization of piperylene and stilbene, the application of an external magnetic field changes both the initial quantum yield for the reaction, and the composition of the photostationary states. In addition, the external field effect was dependent upon the nature of the sensitizer. No firm conclusions as to the origin of the effect were drawn; however, in a later article, an explanation was proposed by Atkins (1973). It was suggested that an exciplex between the excited state of the sensitizer and the olefin should be regarded as having the nature of a radical ion pair. Such a radical pair might possess a significant value of Δg, and hence a magnetic field induced intersystem crossing might occur in a manner analogous to that characteristic

of class III reactions (*vide infra*). The suggestion was supported by a quanti-
tative analysis for an assumed value of Δg; however, as the nature of the
exciplex is in fact unknown, the explanation must be regarded as speculative.

Another related example of class I reaction was reported by Turro *et al.*
(1980c) who observed an external magnetic field effect upon an emulsion
polymerization. Emulsion polymerization (EP) requires an aqueous dis-
persion medium, dispersed droplets of monomer, a micelle-generating deter-
gent, and an initiator. Dibenzyl ketone (DBK) was used as a photochemical
radical initiator for the polymerization of styrene. The DBK is solubilized
in the micelle together with monomer styrene molecules from the dispersed
droplets; hence polymerization is initiated within the micelle. Experiments
were conducted in which a magnetic field was applied at various times after
the start of the polymerization, and it was shown that the field effect lay
exclusively in the initial stage, i.e. when micelles existed. It was found that
the average molecular weight of polymerized styrene could be increased by a
factor of 5 if the reaction was performed in the presence of an applied field
of > 1000 G (Fig. 13). The effect may be explained with the aid of the highly
schematic representation shown in Scheme 5, where the circles represent
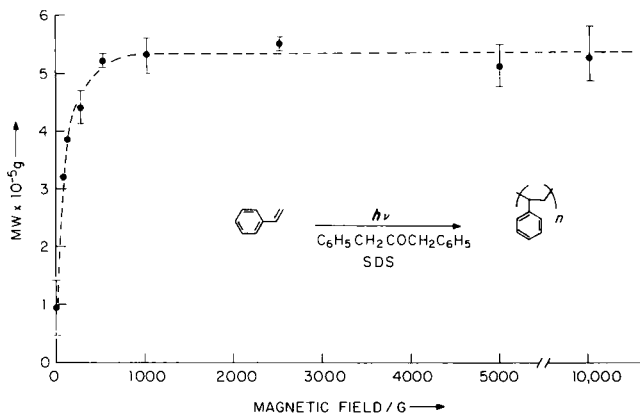micelles, and M monomer styrene molecules.

FIG. 13 Plot showing the effect of an applied magnetic field on the average mole-
cular weight of polystyrene, produced in emulsion polymerization of styrene using
DBK as the photochemical initiator

The molecular weight of the polystyrene depends upon the rates of ter-
mination reactions, which in turn depend upon the availability of terminating
free radicals. Termination by one partner in the initial radical pair requires
an intersystem crossing. This intersystem crossing is in competition with
radical escape into the water phase, and thus the application of an external
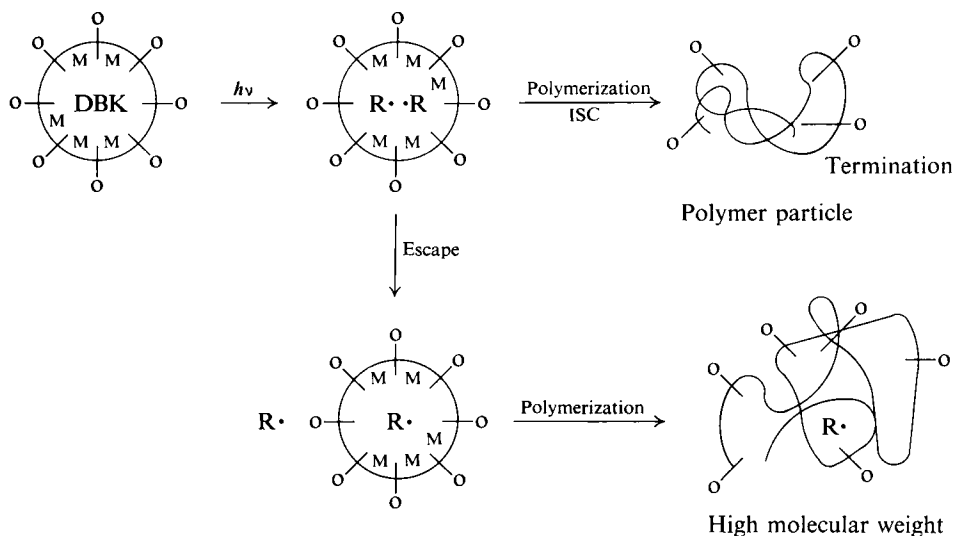
Scheme 5

field allows more radicals to escape. Since radicals in the water are less efficient at terminating the polymerization process which initially proceeds in the micelle, higher molecular weights of polymer are achieved in the presence of an external field.

CLASS II EFFECTS: REACTIONS FOR WHICH THE SINGLET-TRIPLET SPLITTING IS NON-ZERO

Examples of class II reactions are less common than those of class I. The requirement of a substantial non-zero J demands that the radical sites remain a few Å from each other, a situation not encountered for radical pairs in homogeneous or micellar solution. Many short chain biradicals possess this property (Turro and Kraeutler, 1982), but as yet no examples of hyperfine induced magnetic field effects on the chemical reactions of biradicals have been reported.

Photolysis of quinoline N-oxides in alcoholic solvents leads to two products: (i) rearrangement to the lactam via a radical ion pair formed between the quinoline and alcohol, and (ii) isomerization to an oxazepin (Bellamy and Streith, 1976). It has been shown that the ion pair is formed between the quinoline and an alcohol molecule which is hydrogen bonded to the N-oxide oxygen atom (Hata, 1976, 1978). The formation of the oxazepin proceeds via an oxaziridine intermediate, and is magnetic field independent. However, the yield of the lactam was found to be magnetic field dependent

(Hata *et al.*, 1979). It was found that in ethanol, at fields greater than 6 kG, the yield of lactam dropped from 70% to 55% at 10 kG. At higher fields, the yield increased and at 15 kG had returned to 70% (Fig. 14). Hydrogen bonding in the radical ion pair results in significant exchange overlap, which means that intersystem crossing is energetically unfavourable. For this radical pair it is claimed that the singlet state is higher in energy than the triplet state. Thus, in the presence of a sufficiently high magnetic field, the T_+ sublevel is raised in energy, due to the Zeeman interaction, so that at a certain field, S_0 and T_+ become energetically degenerate. Thus, at this field, intersystem crossing between S_0 and T_+ is possible due to hyperfine interactions. In this case, resonant interaction is observed at 10 kG, which gives the value of $2J$ for this radical pair. Support for the interpretation came from the following consideration. It was argued that the distance between the radical pair centres and thus the extent of exchange overlap for quinoline N-oxide and a given set of alcohols will depend upon the pK_a-value of the alcohol. It was found that the minimum yield of lactam occurred at 7 kG for t-butyl alcohol and at ~ 18 kG for methanol. Thus, the magnetic field required for the resonance condition is dependent upon the distance between the radical centres.
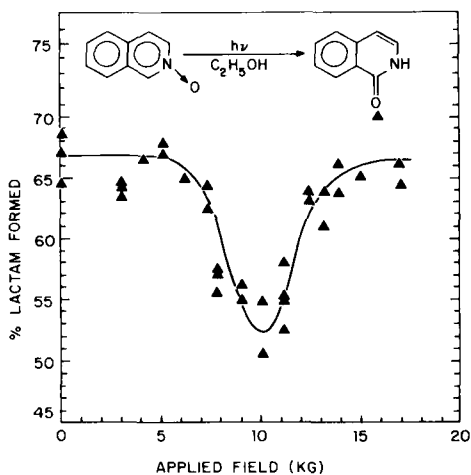

FIG. 14   Plot showing the effect of an external magnetic field on the yield of lactam formed during photolysis of quinoline N-oxide in ethanol. The maximum magnetic field effect occurs when the S-state of the intermediate radical ion pair is degenerate with the T_+-state

Similarly, the photosubstitution reaction (20) of 4-methylquinoline-2-carbo-nitrile is affected by an external magnetic field (Hata and Hokawa, 1981). The reaction is again assumed to proceed *via* an initially singlet radical

$$(20)$$

[5]   [6]
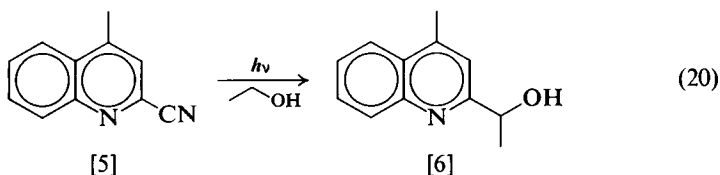
ion pair which may (*i*) intersystem cross to give a triplet pair, followed by diffusive separation and ultimate regeneration of starting materials, or (*ii*) undergo a hydrogen-atom transfer from the alcohol to the quinoline nitrogen, followed by formation of the substitution product. In fact, a plot of the yield of the cage product [6] as a function of field reveals a minimum at a value of 10 kG. Again the interpretation is that at this field a resonance between S and T_+ occurs, so that hyperfine induced intersystem crossing is enhanced, and thus the yield of cage product decreases.

CLASS III EFFECTS: REACTIONS FOR WHICH THE Δg-MECHANISM FOR INTERSYSTEM CROSSING IS DOMINANT

The occurrence of Δg magnetic field effects on chemical reactions requires either a large Δg ($> 10^{-2}$ to 10^{-3}) or a very large magnetic field ($> 10^5 G$); the former is not often encountered in carbon-based radicals, and the latter is difficult to achieve in the laboratory. Even so, magnetic field effects which have been attributed to the Δg-mechanism have been reported. They usually accompany Zeeman effects and are observed at higher field strengths.

The pyrene-sensitized photoisomerization of decafluorostilbene is influenced by an external magnetic field in a manner similar to that described earlier for *trans*-stilbene (Leshina *et al.*, 1980). At low fields, intersystem crossing from a singlet radical ion pair to a triplet pair is inhibited; this reduces the efficiency of formation of the free stilbene triplet, and hence lowers the probability of *trans* → *cis* conversion. However, at fields above 10 kG, the yield of *cis*-decafluorostilbene from *trans*-decafluorostilbene increases relative to that at fields in the order of 1 kG, an effect not observed for stilbene itself. The decafluorostilbene-pyrene radical ion pair has a reported Δg of 2×10^{-3}, compared to that for stilbene-pyrene radical ion pair of 2×10^{-4}. Since the rate of Δg-promoted S → T_0 intersystem crossing depends directly upon the value of Δg, a greater effect would be expected for *trans*-decafluorostilbene. Thus, at fields of 10 kG, the rate for the new mechanism of intersystem crossing for this stilbene becomes competitive with the rate of back electron transfer within the singlet ion pair. This effect results in more probable formation of *trans*-decafluorostilbene triplet and hence a higher yield of *cis*-decafluorostilbene.

TABLE 3

Effect of ultrahigh magnetic field on cage reactions of dibenzyl ketones photolyzed in HDTCl micelles[a]
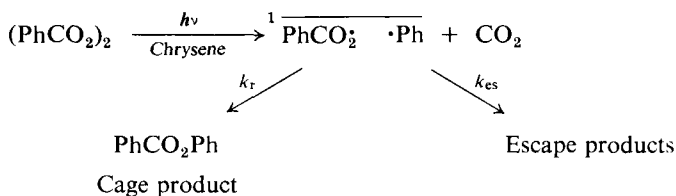
Radical pair	Field strength/G	% Cage products	Δg
p-CH$_3$—PhCH$_2$ $\cdot$ $\cdot$ CH$_2$Ph	0	48	3×10^{-5}
	14,500	25	
	145,000	21	
p-ClPhCH$_2$ $\cdot$ $\cdot$ CH$_2$Ph	0	52	5.5×10^{-4}
	14,500	31	
	145,000	37	
p-BrPhCH$_2$ $\cdot$ $\cdot$ CH$_2$Ph	0	58	2.1×10^{-3}
	14,500	58	
	145,000	57	
PhCH$_2$ $\cdot$ $\cdot$ CH$_2$Ph	0	32	0
	14,500	16	
	145,000	13	
PhCO $\cdot$ $\cdot$ C(CH$_3$)$_2$Ph	0	30	2.2×10^{-3}
	10,000	19	
	145,000	23	

[a]Turro et al., 1982a

The use of ultrahigh laboratory magnetic fields has enabled the observation of Δg effects in the systems studied by Turro et al. (1982a). Dibenzyl ketones which were substituted in the 4-position of a benzene ring were photolyzed in HDTCl micelles and the cage effect on the diphenylethane products were determined as described earlier. The value for the cage effect was determined in the presence of magnetic fields of zero, 14,500, and 145,000 G. The results are summarized in Table 3. For methyl-substituted DBK which has a small Δg, the effect of the ultrahigh field is similar to that observed for the parent compound, i.e. no change is noted. However, for the case of the chloro-substituted radical, Δg is relatively large and an increase in the percentage of cage reaction occurs upon going from high fields to ultrahigh fields. This effect is also observed for photolysis of 1,2-diphenyl-2-methylpropanone (Table 3), where an increase in the cage effect is noted at ultrahigh laboratory magnetic fields. These results were interpreted as evidence for a Δg-mechanism for intersystem crossing in these two radical pairs. Thus, although inter-system crossing, and hence formation of cage products, is inhibited at low fields due to the Zeeman effect, at high fields the $T_0 \rightarrow S$ crossing is enhanced directly as a result of the high applied field. Of interest are the results of experiments performed using 4-bromo DBK. In this case, the benzyl radical pair possesses the largest value of Δg, but the percentage of cage reaction is the same at low field and high field as that measured at zero field. These

results were interpreted to mean that a new mechanism for intersystem crossing now dominates, i.e. spin-orbit coupling. This result is consistent with the observation that the ^{1}H CIDNP spectrum of photoexcited 4-bromo-DBK is very weak compared to those from DBK and 4-chloro-DBK.

The singlet sensitized decomposition of dibenzoyl peroxide in toluene has been shown to be magnetic field dependent (Tanimoto et al., 1976; Sakaguchi et al., 1980). The reaction may be summarized simply as shown in Scheme 6. Chrysene was used as a singlet sensitizer for the reaction; hence the initial radical pair is a benzoxyl ·· phenyl pair in a singlet state. Phenyl benzoate is the cage product. Radicals which escape the solvent cage result in a variety of products, many of which involve the solvent toluene. The value of Δg for the benzoxyl ·· phenyl radical pair is quite large (~ 0.01), and hence a field effect is expected. Experimentally, it is found that the yield of phenyl benzoate (cage product) decreases by 8% in the presence of a magnetic field of up to 43 kG. A corresponding but small (2%) increase in the out of cage products is observed. An analysis of the data according to a theoretical model allows assignment of the mechanism of the effect to a Δg-phenomenon, although in the later paper (Sakaguchi et al., 1980) more complex effects are claimed.

$$(PhCO_2)_2 \xrightarrow[\text{Chrysene}]{h\nu} {}^1\overline{PhCO_2^{\cdot} \quad \cdot Ph} + CO_2$$

$$\swarrow k_r \qquad\qquad\qquad k_{es} \searrow$$

PhCO$_2$Ph   Escape products

Cage product

Scheme 6

Thermolysis of certain 1,4-endoperoxides of aromatic compounds produces molecular oxygen and the parent hydrocarbon quantitatively (Rigaudy and Basselier, 1971). From a study of the activation parameters it has been shown that these reactions proceed by two pathways: (i) a concerted mechanism in which singlet oxygen is formed quantitatively, and (ii) a diradical mechanism in which both excited singlet ($^1O_2$) and ground state triplet ($^3O_2$) oxygen are produced (Turro et al., 1979a). Since the spin states of a diradical are entirely analogous to those of a radical pair (Turro and Kraeutler, 1982), it is expected that only the diradical pathways will be influenced by a magnetic field. A simplified diradical mechanism for endoperoxide thermolysis is shown in Scheme 7 (Turro and Chow, 1979). Thermolysis is presumed to lead to an initially singlet diradical (^1D), and this species may either fragment to yield singlet oxygen (k_r^1), or undergo intersystem crossing (k_{ISC}) and fragment (k_r^3) to yield triplet oxygen. Since the g-values for peroxy radicals are large (typically ~ 2.01) (Berndt et al., 1977), these diradicals should have

$$^1D \qquad\qquad ^3D$$

$$\downarrow k_r^1 \qquad\qquad \downarrow k_r^3$$

$$^1O_2 \qquad\qquad ^3O_2$$
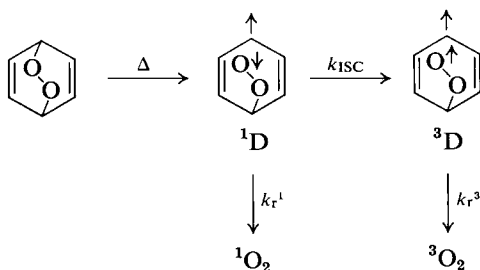
Scheme 7

large values of Δg. Hence at sufficiently high magnetic fields, the Δg-effect will increase k_{ISC} relative to k_r^1. A higher yield of $^3O_2$ and a lower yield of $^1O_2$ are therefore expected when endoperoxides, which decompose *via* diradicals, are thermolyzed in a magnetic field. Furthermore, no effect of magnetic field is expected if a concerted mechanism for decomposition is involved. In Fig. 15 are shown plots of $^1O_2$ yield as a function of magnetic field for thermolysis of two endoperoxides (Turro and Chow, 1979). Compound [7] has been shown to decompose by the diradical mechanism and compound [8] by the concerted mechanism. A decrease in $^1O_2$ yield is found for endoperoxide [7] in the range 9,000–15,000 G, whereas for [8] no change is observed. These results support the assignment of a Δg-mechanism for magnetic field induced intersystem crossing for these diradicals.
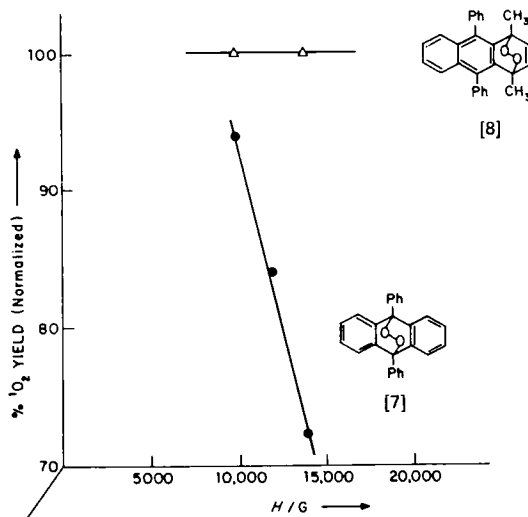

FIG. 15   Magnetic field effects on the yield of singlet oxygen formed upon thermolysis of a 9, 10- and a 1,4-endoperoxide

CLASS IV EFFECTS: MAGNETIC ISOTOPE EFFECTS

Although magnetic isotope effects may be observed in the presence of labor-
atory fields, for the sake of simplicity and clarity we shall consider first the
situation in the absence of any applied field. As for magnetic field effects,
essential requirements for the observation of significant magnetic isotope
effects (Lawler and Evans, 1971; Buchachenko, 1976) are (i) a competition
for a spin correlated radical pair between magnetic isotope-induced inter-
system crossing (which leads to a capture pathway) and a spin dependent
escape pathway, and (ii) a set of experimental conditions that allows the
magnetic isotopes to exert a significant influence on the rate of intersystem
crossing in the spin correlated radical pair. Thus, as for magnetic field effects,
magnetic isotope effects are generally very small or negligible in homogeneous
solution, but may become significant in microheterogeneous environments
such as micelles.

TABLE 4

Some properties of common isotopes

Nucleus	γ^a	$\mu_N{}^b$	I (spin)	Natural abundance (%)
^{1}H	27,000	2.79	1/2	100
^{2}H	4100	0.86	1	0.016
^{3}H	—	2.98	1/2	0
^{12}C	0	0	0	99
^{13}C	7000	0.70	1/2	1.11
^{14}C	0	0	0	0
^{16}O	0	0	0	100
^{17}O	−3600	−1.9	5/2	0.04
^{18}O	0	0	0	0.20
^{117}Sn	−9600	−0.99	1/2	7.7
^{119}Sn	−10,000	−1.04	1/2	8.7

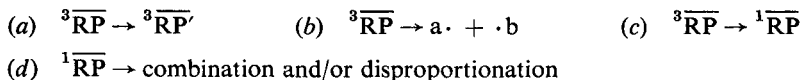[a]Magnetogyric ratios in radians $s^{-1}G^{-1}$.   [b]Nuclear magnetic moments in erg G^{-1}

Table 4 lists the magnetic properties of elements that commonly occur in
organic compounds. Consider first the isotopic triad ^{1}H, ^{2}H, and ^{3}H. The
magnetic spins and magnetic moments of ^{1}H and ^{3}H are identical, although
their masses differ by a factor of three. Thus, there is no possibility of differ-
entiating radical pairs possessing ^{1}H and ^{3}H based on their magnetic proper-
ties. On the other hand, ^{1}H and ^{2}H differ both in terms of their spin (^{1}H,
spin = 1/2; ^{2}H, spin = 1) and their magnetic moments (ratio of magnetic
moments for ^{1}H/^{2}H = 3). The magnetogyric ratio (γ), the ratio of the magnetic
moment to the spin angular momentum (Carrington and McLauchlan, 1967),
is the important quantity. The value of γ for ^{1}H is six times that of ^{2}H. Thus,

the hyperfine coupling of ^{1}H is six times larger than that of ^{2}H. The difference in the hyperfine couplings represents a mechanism for the differentiation of radical pairs possessing ^{1}H or ^{2}H. Consider next the ^{16}O, ^{17}O, and ^{18}O triad. The even-numbered mass isotopes of oxygen possess no spin and are non-magnetic, while the odd-numbered mass isotope possesses a spin of 1/2 and is magnetic. Thus, it is again conceivable that radical pairs possessing ^{16}O (or ^{18}O) may be differentiated from those containing ^{17}O by magnetic isotope effects. From this discussion it can be seen that the magnetic isotope effect may serve as a novel means of isotopic separation or enrichment, i.e. as a method which employs magnetic properties rather than mass properties as the basis for the separation (Buchachenko *et al.*, 1981; Buchachenko, 1977).

As for magnetic field effects, magnetic isotope effects are expected to be maximal in closed volume reaction environments such as micelles and for initial triplet spin-correlated radical pairs (Turro and Kraeutler, 1980; Turro, 1983; Closs, 1971; Sterna *et al.*, 1980; Tarasov *et al.*, 1981).

The reactivity of a radical pair (RP) within a solvent cage $(\overline{RP})$ depends critically on the spin state of the pair; a singlet RP ($^1\overline{RP}$) within a solvent cage is very reactive toward combination and disproportionation reactions, but triplet RP's in a solvent cage ($^3\overline{RP}$) are completely unreactive toward such reactions. The options (Scheme 8) open to a $^3\overline{RP}$ in a chemically inert solvent are (*a*) chemical modification of one (or both) of the components of the pair to produce a structurally different triplet pair ($^3\overline{RP'}$), (*b*) relative diffusion of the pair out of the solvent cage, and (*c*) intersystem crossing to produce a reactive singlet RP. The general rule concerning the differing reactivities of $^1\overline{RP}$ and $^3\overline{RP}$ is based on the premise that the time of reaction of a caged singlet RP is too short for a change of electronic spin multiplicity.

(*a*) $^3\overline{RP} \rightarrow {}^3\overline{RP'}$ (*b*) $^3\overline{RP} \rightarrow a\cdot + \cdot b$ (*c*) $^3\overline{RP} \rightarrow {}^1\overline{RP}$

(*d*) $^1\overline{RP} \rightarrow$ combination and/or disproportionation

Scheme 8

In Scheme 8, path (*b*) provides an *escape* pathway for pairs that possess non-magnetic spins, and path (*c*) provides a *capture* for the pairs that possess magnetic spins. A strategy for controlling the reactions of RP's with nuclear spins can now be developed. If the nuclear spins communicate with the electron spin *via* nuclear-electronic hyperfine-induced intersystem crossing of a RP, then the reactivity of the RP depends on the nuclear-electronic hyperfine coupling. As a general example, consider (Fig. 16) two RP precursors, a* — b and a — b, which differ only in isotope composition (* refers to the occurrence of magnetic nuclei in a fragment of the RP). Suppose
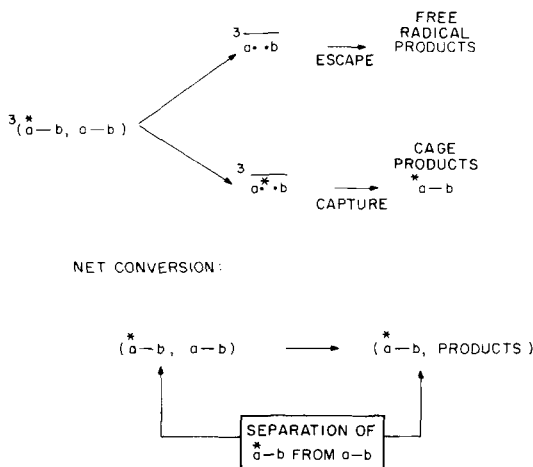
FIG. 16   Diagram which illustrates the concept of the magnetic isotope effect on chemical reactions. Triplet radical pairs which contain a magnetic nucleus (* in the diagram) are more likely to undergo recombination (capture) reactions. Triplet radical pairs which do not contain a magnetic nucleus are more likely to undergo (escape) product forming reactions

now that both precursors are cleaved into a caged triplet RP, $^3\overline{\text{a} \because \text{. b}}$ and $^3\overline{\text{a} \cdot\cdot \text{b}}$, respectively, Of the two, $^3\overline{\text{a} \because \text{. b}}$ will convert more rapidly into singlet $^1\overline{\text{a} \because \text{. b}}$ *because the magnetic nuclei in* a* *provide a mechanism for intersystem crossing which is completely absent in* $^3\overline{\text{a} \cdot\cdot \text{b}}$. If a singlet RP undergoes a cage recombination reaction, then a* — b will be reformed faster than a — b. This means that *as the reaction proceeds, the system will become enriched in the reagent containing magnetic nuclei. In principle, such a system could lead to complete separation of the isotopic materials of* a* — b *and* a — b, *if the escape process occurred for all pairs that did not contain magnetic spins and if the capture process occurred for all pairs containing magnetic spins.*

   We may now consider a simple hydrodynamic model which schematically displays the essence of the capture/escape concept (Fig. 17). Suppose a fluid may be pumped into two separate receptacles that possess a switch which prevents the fluids in the two containers from mixing. Both containers possess holes which allow the fluids to be removed. Consider now the analogy of fluid pressure and chemical potential. The fluid on the left is analogous to singlet states producing singlet radical pairs and the fluid on the right is analogous to triplet states producing triplet radical pairs. The switch is analogous to the magnetic effects which allow mixing of the singlet and triplet radical pairs. If one starts from the triplet, and if hyperfine interactions allow
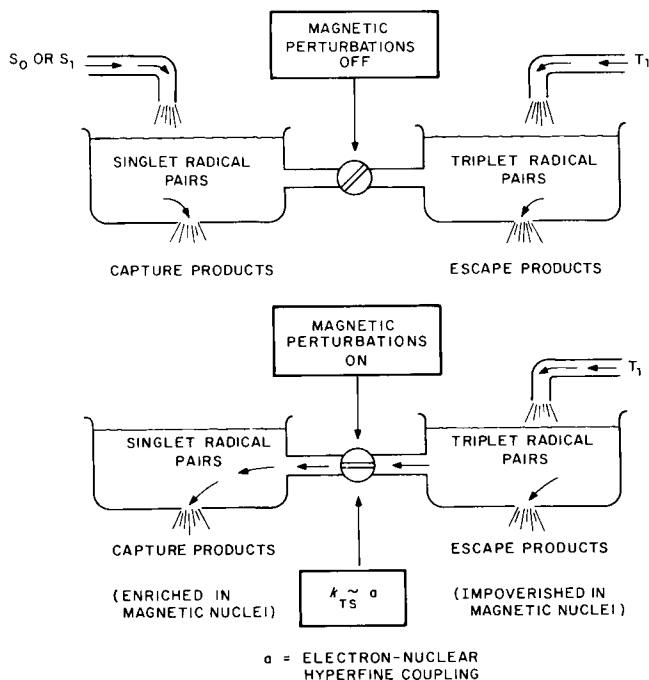
FIG. 17   Schematic illustration of the effect of the perturbations induced by magnetic nuclei on the relative amounts of capture and escape reactions for radical pairs. The number of capture reactions for triplet radical pairs with a magnetic nucleus increases as a consequence of the magnetic perturbations

triplet and singlet to mix, the "flow" of triplet radical pairs into the singlet container is apparent. The rates of mixing, capture, and escape all contrive to determine the efficiency of the processes.

For a high efficiency of isotopic separation, two important criteria must be met: (i) the hyperfine interactions in $^3\overline{\text{a} \ddot{\cdot} \cdot \text{b}}$ must be large enough to allow for the possibility that intersystem crossing to $^1\overline{\text{a} \ddot{\cdot} \cdot \text{b}}$ can be determined mainly by nuclear electron hyperfine interactions, and (ii) the formation of free radical products (chemically or by modification of the RP) from $^3\overline{\text{a} \cdot \cdot \text{b}}$ must occur more efficiently than intersystem crossing to $^1\overline{\text{a} \cdot \cdot \text{b}}$. In turn, in order for these criteria to be met, certain space/time conditions must exist: (i) the caged RP $^3\overline{\text{a} \ddot{\cdot} \cdot \text{b}}$ must be able to use the hyperfine interactions fully by being able to have the radical fragments separate in space to a distance such that the singlet-triplet splitting is of the order of or smaller than the hyperfine interaction, and (ii) the time of separation must be appropriate for maximal intersystem crossing induced by hyperfine interactions.

Although these conditions are stringent, numerous systems have been discovered for which the efficiency of isotopic separation by the magnetic isotope effect far exceeds that for separation by the mass isotope effect. In the following sections examples are given of magnetic isotope effects involving carbon, hydrogen, oxygen, and tin.

Magnetic isotope effects involving carbon nuclei

As a specific example of magnetic isotope effects, let us focus attention on the combination products from photolysis of DBK and PMAP (Fig. 12). These products are formed from the triplet correlated radical pairs (^{3}RP) after intersystem crossing to the singlet correlated radical pair (^{1}RP). If ^{13}C nuclei in ^{3}RP assist in the formation of ^{1}RP, then the rate and the efficiency of the ^{3}RP $\rightarrow$ ^{1}RP process will depend on the occurrence (or non-occurrence) of ^{13}C nuclei in the radical fragments. Suppose that a given ^{3}RP possess a ^{13}C nucleus which is coupled by the hyperfine interaction to one of the odd electrons. This ^{3}RP will enjoy a faster intersystem crossing rate than a ^{3}RP that contains only ^{12}C nuclei, i.e. the ^{13}C nuclei can promote the ^{3}RP $\rightarrow$ ^{1}RP process *via* both the spin rephasing ($T_0 \rightarrow S$, Fig. 6a) and spin flipping ($T_+ \rightarrow S$ or $T_- \rightarrow S$, Fig 6b) mechanisms. The recombination process provides a "capture" pathway for ^{3}RP containing ^{13}C nuclei and loss of carbon monoxide provides an "escape" pathway for ^{3}RP containing ^{12}C nuclei (Scheme 9).
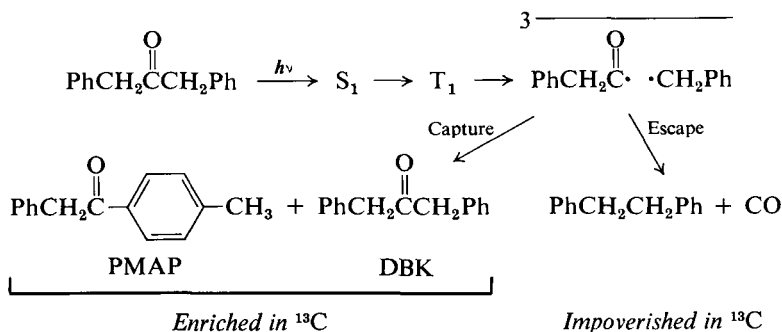
Scheme 9

The occurrence of a ^{13}C magnetic isotope effect in the ^{3}RP from DBK leads to the following predictions: (*i*) the combination products, DBK and PMAP (Fig. 12), will be enriched in ^{13}C relative to the starting ketone; (*ii*) the extent of ^{13}C enrichment at the various carbon atoms of DBK and PMAP will depend on the magnitude of the ^{13}C hyperfine couplings of the various carbon atoms in ^{3}RP; (*iii*) the efficiency of ^{13}C enrichment in DBK and PMAP will be magnetic field dependent, the efficiency decreasing at high fields
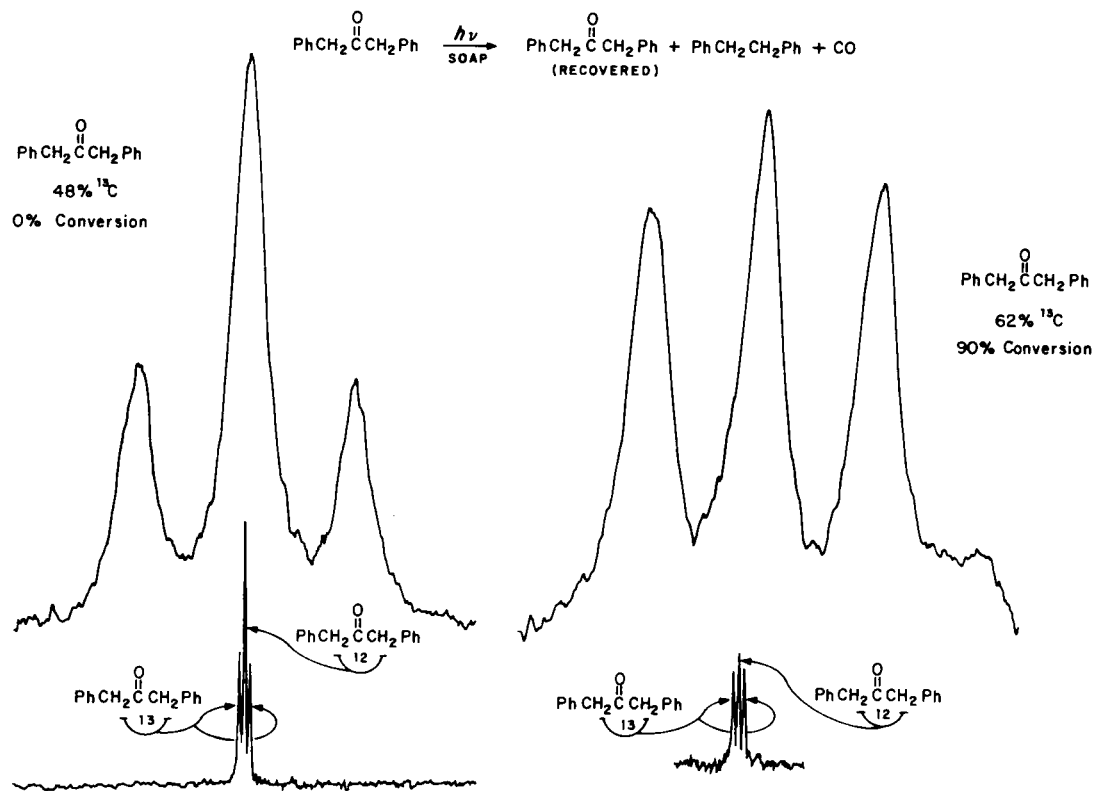
FIG. 18 ¹H nmr spectra of ¹³C-labelled dibenzyl ketone. (*Left*) starting ketone. (*Right*) ketone recovered after 90% photolysis in micellar solution

(when T_+ and T_- are "shut off" from intersystem crossing because of Zeeman splitting); (iv) the efficiency of ^{13}C enrichment at ultrahigh fields will approach zero and the magnetic isotope effect will disappear (when the ΔgH-mechanism dominates the $^3RP \rightarrow {}^1RP$ process which then no longer depends on the occurrence of magnetic nuclei in ^3RP).

All four of these expectations have been confirmed experimentally (Turro, 1981, 1983; Turro and Kraeutler, 1980). Figure 18 demonstrates the prediction of ^{13}C enrichment in DBK recovered from the micellar photolysis of DBK. The ^1H nmr spectrum of DBK that has been synthetically enriched to 48% in ^{13}C at the carbonyl carbon (natural abundance of ^{13}C is 1.1% per carbon atom) is shown at the left of Fig. 18. A very sensitive test for the ^{13}C enrichment of the carbonyl of DBK is available from integration of the ^{13}C satellites in the ^1H nmr spectrum (Turro et al., 1981b). The methylene protons of DBK (Fig. 18) with a ^{12}C carbonyl appear as a singlet (at 3.66 ppm, $CHCl_3$, Me_4Si as internal reference); a doublet centred at the same chemical shift with $J_{^{13}C,H} = 6.5\ Hz$ is caused by ^{13}C-proton coupling when ^{13}C is contained in the carbonyl group. Integration over the singlet and doublet signals allows determination of the ^{13}C content of the carbonyl of DBK. Thus, from the satellite method, $62 \pm 4\%$ ^{13}C is computed to be in the recovered DBK (after 91% conversion). For the DBK recovered after 91% conversion, a quantitative agreement exists between the mass spectrometrically determined mass increase and the ^{13}C-enrichment of the carbonyl of DBK determined by ^1H nmr spectroscopy. After mass spectroscopy and ^1H nmr analysis, these samples of DBK were subjected to ^{13}C nmr analysis, which also established qualitatively that the predominant ^{13}C enrichment occurs in the carbonyl of DBK (the relative increase of the carbonyl signal corresponds to a $60 \pm 5\%$ ^{13}C content). These experiments demonstrate that recovered DBK becomes enriched in ^{13}C as a result of photolysis of DBK in micelles and provide strong evidence that there is a magnetic spin isotope effect in the photolysis of DBK in micellar systems. In contrast, the photolysis of DBK in non-viscous homogeneous solvents (e.g. benzene) results in a much less efficient ^{13}C enrichment in the recovered DBK (Turro et al., 1982b).

In the photolysis of DBK, if ^{13}C nuclear spins control intersystem crossing from ^3RP to ^1RP, starting from natural abundance ^{13}C ($\sim 1\%$) at each carbon, the ^{13}C enrichment at the various distinguishable carbon atoms in the combination products will be related to the magnitude of the ^{13}C hyperfine constant, a_C, for each of the corresponding carbon atoms in ^3RP.

Table 5 lists the measured or estimated values of a_C for the eleven different carbons in ^3RP (see Fig. 19 for numbering system) (Turro et al., 1982b). If, as expected for freely diffusing radical pairs, the ^{13}C enrichment increases monotonically with a_C, it is apparent from Table 5 that the ordering of ^{13}C enrichment should be C–1 > C–10 > C–11 > aromatic C. According to

TABLE 5

Relative ^{13}C isotope ratios for 1-phenyl-4-acetophenone by ^{13}C nmr spectroscopy[a]

Carbon[b]	δ_{C}' ppm[c]	S[d]	a_C/G
1	197.40	1.23 ± 0.01	+124
2	144.12	(1.00)	−14
3	134.93	0.99	0
4	134.25	0.99	+11
5	129.59	0.99	0
6	129.48	1.01	+12
7	128.91	0.99	−9
8	128.79	0.99	0
9	126.95	0.98	0
10	45.60	1.17	+51
11	21.84	1.06	+24

[a] Turro *et al.*, 1982b
[b] See Fig. 19 for number system
[c] Chemical shifts relative to $\delta_C^{CHCL_3} = 77.27$ ppm. Assignments were made by using selective ^{1}H decoupling
[d] Ratio of ^{13}C nmr intensities for analytical and standard samples divided by the ratio for C–2

the mechanism for photolysis of DBK given in Fig. 12, 1-phenyl-4-methyl-acetophenone (PMAP) is a combination product which both results after $^3RP \rightarrow {}^1RP$ and which preserves the memory of each distinct carbon atom of ^3RP in its final structure.

Although mass spectroscopic analysis allows determination of the global ^{13}C enrichment in PMAP, the measurement of ^{13}C enrichment at each carbon is best made by a magnetic resonance method. ^{13}C Satellite intensities in the ^{1}H nmr spectrum, for example, were used as a complement to mass spectroscopy for monitoring the ^{13}C content of specifically labelled DBK and PMAP samples. However, ^{13}C nmr spectroscopy has the advantage that specific ^{13}C labelling is not required, because small deviations from natural abundance may be determined directly by comparing peak intensities from the sample of interest with those from a standard. The relative enrichments for PMAP obtained in this way are in Table 5.

The data in Table 5 may be summarized as follows: (*i*) Statistically significant enrichments are obtained for C–1, C–10, and C–11 in the expected order C–1 > C–10 > C–11; (*ii*) The ^{13}C contents of the other eight carbons varied in this particular sample by <2% from those of the natural abundance sample. The enrichment factor S (*vide infra*), however, seems to depend somewhat non-linearly on a_C. For example, C–10 seems to be over-enriched
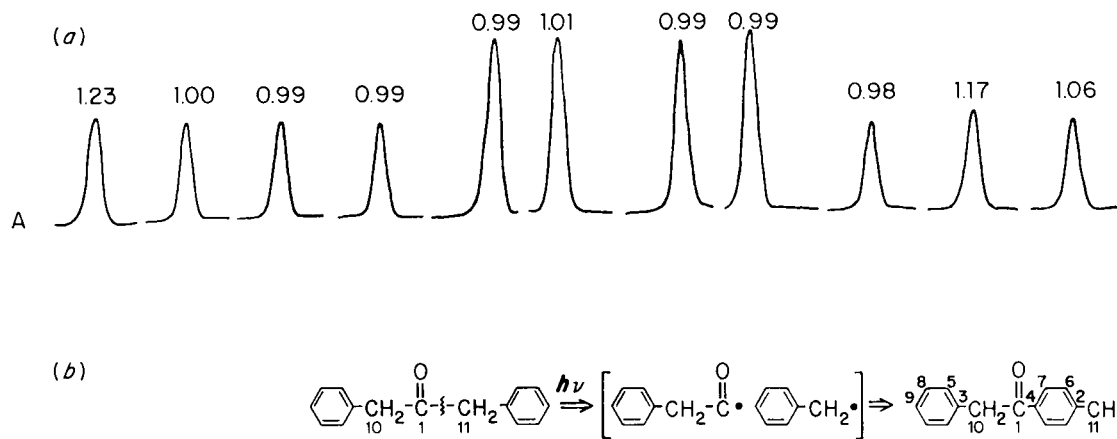
FIG. 19 ^{13}C nmr analysis of the ^{13}C-content of 1-phenyl-4-methylacetophenone produced by photolysis of DBK in micellar solution. (*a*) Integration according to chemical shifts of the ^{13}C atoms. (*b*) Structure showing numbering system for the ^{13}C atoms

and C–2 under-enriched relative to the magnitudes of their hyperfine coup-
lings. The data nevertheless are in good qualitative agreement with the ex-
pectations for a predominant nuclear spin, rather than mass, isotope effect
for the formation of PMAP.

Bernstein (1952, 1957) has shown that for competitive first order isotopic
reactions the residual unconverted starting material becomes exponentially
enriched in the slower reacting isotope. As a result, if the isotopic rate factor
is substantial and if the reaction is run to high conversion, the recovered
material may become significantly enriched in the slower reacting isotope. In
the case of the photolysis of DBK, if we consider only the $^{12}C/^{13}C$ competitive
isotopic reactions, then residual, unconverted DBK will become enriched in
^{13}C if molecules containing this isotope proceed to products at a slower rate
than molecules that contain ^{12}C. A parameter α may then be defined as the
single stage separation factor, and can be computed from the measurable
quantities S, the overall separation factor (related to the ^{13}C content of
product relative to starting material), and f, the fractional conversion (Duncan
and Cook, 1968). For practical cases the appropriate approximate formula
for calculation of α is given by (21). Thus, one can measure the ^{13}C content of

$$\log\ S = \frac{\alpha - 1}{\alpha}\ [-\log\ (1\ -f)]$$

(21)

the recovered DBK, compare it to the ^{13}C content of the initial DBK, com-
pute S and then plot $\log S$ vs $-\log (1\ -f)$. The slope of such a plot, if linear,
is identified as $(\alpha - 1)/\alpha$. Experimental plots are shown in Fig. 20.

The striking results which are observed are: (i) the value of α for photolysis
of DBK in a micellar system is enormously higher than that for photolysis
of DBK in a non-viscous homogeneous solvent, and (ii) the value of α for
photolysis of DBK in a micellar system is strongly magnetic field dependent
(Turro et al., 1981b). The value of $\alpha = 1.03$ for benzene is of the order of the
$^{13}C/^{12}C$ mass isotope effects that have been reported. Thus, the value of
$\alpha = 1.42$ (global enrichment, normalized to a single carbon atom) represents
a magnetic effect far beyond any previously observed for $^{13}C/^{12}C$ mass isotope
effects.

The observation that (21) is obeyed experimentally provides a useful
parameter, α, for quantitative discussion of enrichment efficiency. Consider-
ation of Fig. 21 allows an appreciation of the relationship of α to $^{13}C/^{12}C$
separation efficiency. As α increases, the separation factor $(^{13}C/^{12}C)_f$ increases
for any given extent of reaction. For example, for 99 % conversion, if $\alpha = 1.05$,
1.5, 3.6, or 20, then $(^{13}C/^{12}C)_f$ will equal 1.4%, 5%, 19%, 37%, and 50%,
respectively. Suppose these α-values refer to enrichment at a single carbon.
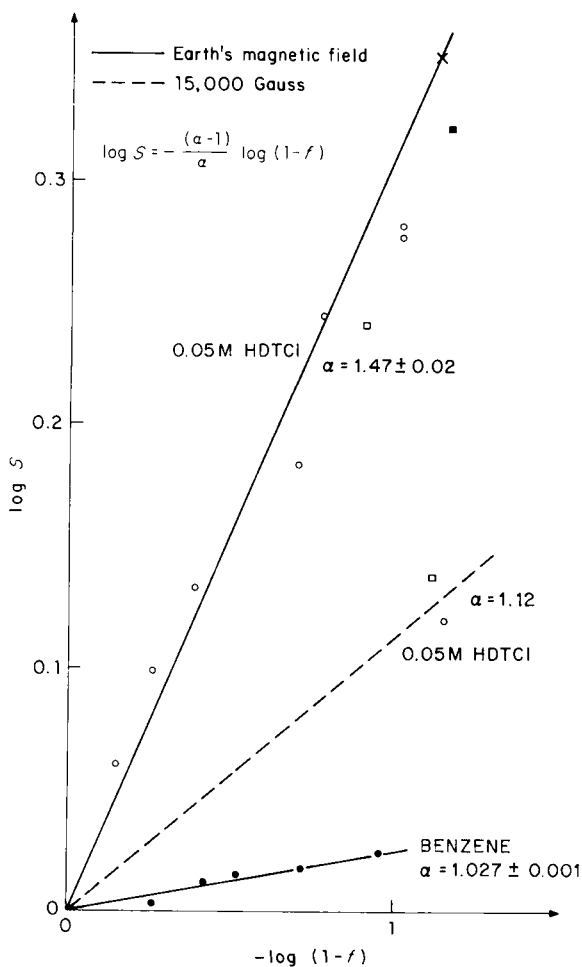Then, starting with natural abundance material for which $(^{13}C/^{12}C)_f = 1/99$,

FIG. 20   Typical experimental plots of log S vs $-\log(1-f)$ for the photolysis of DBK. The slope of such plots allows calculation of α, the isotopic enrichment factor

for $\alpha = 20$, this carbon will possess $(^{13}C/^{12}C)_f = 1/1$ at 99% conversion. Putting it another way, starting with a mole of natural abundance material, the amount labelled at the pertinent carbon atom will be ~ 0.01 mole, and the final residual material after 99% conversion (0.01 mole) will contain ~ 0.005 mole of labelled compound.

It was stated above that the efficiency of enrichment should decrease at ultrahigh magnetic fields. Indeed, photolysis of DBK in an applied field of
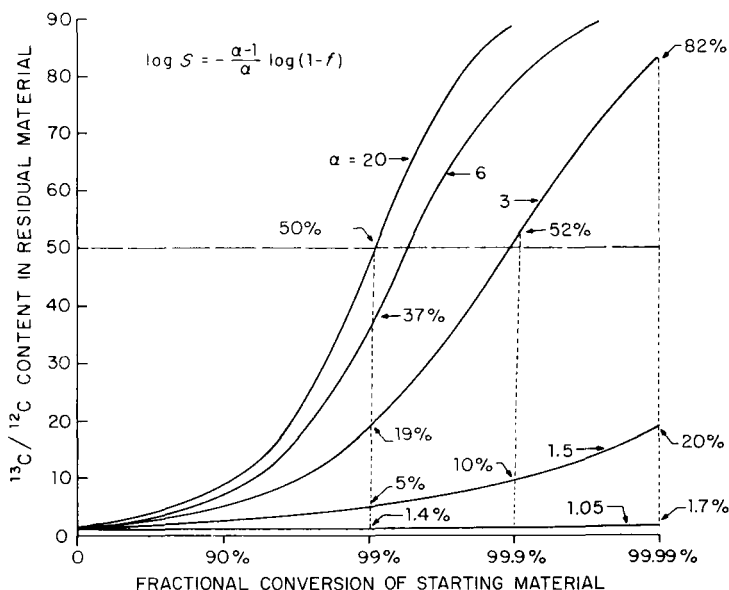
FIG. 21   Relation of experimental ^{13}C enrichment (calculated for a single carbon atom) as a function of conversion for the photolysis of DBK. The family of curves are generated by using differing values of α

150,000 G results in $\alpha = 1.02$, a value comparable to that expected for a $^{12}C/^{13}C$ *mass* isotope effect.

Several other qualitative predictions of the magnetic isotope effect on ^3RP in the micellar photolysis of DBK have been confirmed (Turro *et al.*, 1981a,b): (*i*) the quantum yield of disappearance of ^{12}C-DBK should be *greater* than the quantum yield of disappearance of ^{13}C-containing DBK because recombination of ^3RP will be more efficient for ^{13}C-containing ^3RP, thereby causing more efficient regeneration of DBK and a lower *net* reaction efficiency; (*ii*) the cage effect for benzyl radical pairs produced by loss of CO from ^3RP will be higher when ^{13}C occurs at the methylene carbon of DBK (but not when ^{13}C occurs at the carbonyl carbon of DBK). Prediction (*i*) is confirmed by the observation that the quantum yields for disappearance of DBK (natural abundance), DBK-^{13}CO and DBK-$^{13}CH_2$ were found to be 0.30, 0.22, and 0.25, respectively. Prediction (*ii*) is confirmed by the observation that the cage effect of benzyl radical coupling for DBK-$^{13}CH_2$ is 43%, while the cage effect for benzyl radical coupling of DBK (natural abundance) is 30%.

As discussed above, the decomposition of dibenzoyl peroxide is subject to magnetic field effects (Scheme 6). A ^{13}C magnetic isotope effect has been

demonstrated (Sagdeev *et al.*, 1977a) in the triplet sensitized decomposition of dibenzoyl peroxide (Scheme 10). Phenyl benzoate, the recombination product, was prepared by irradiation of a CCl_4 solution of dibenzoyl peroxide containing acetophenone as a triplet sensitizer until $> 95\%$ of the starting material had reacted. A low chemical yield (*c.* 3%) of phenyl benzoate was produced and analyzed for ^{13}C content by quantitative ^{13}C nmr spectroscopy.
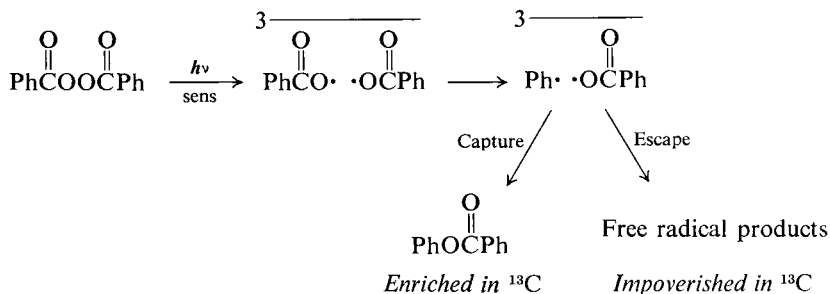
Scheme 10

It was found that the ^{13}C content at the *ipso*-position of the phenyl group bound directly to oxygen in phenyl benzoate possessed a ^{13}C content which was 23% higher than that found in the other positions of the product molecule. The thermal decomposition of dibenzoyl peroxide also produces phenyl benzoate as a product. However, in this case no ^{13}C enrichment was found for any carbon atom in the phenyl benzoate.

These results are readily explained by the hypothesis that triplet sensitization produces a triplet radical pair (Scheme 10) which is capable of the ^{13}C capture and ^{12}C escape processes needed to produce a magnetic isotope effect, but that the thermolysis produces a singlet radical pair which undergoes cage reaction too rapidly to allow hyperfine interactions to influence the reactivity of the radical pair. The selective ^{13}C enrichment at the *ipso*-position of the product is consistent with the large ^{13}C hyperfine coupling (> 1000 G) of the 1-position of phenyl radicals (Berndt *et al.*, 1977).

Magnetic isotope effects involving hydrogen nuclei

Examples of magnetic isotope effects involving deuterium have been observed in the photolysis of DPMP (Scheme 3) (Turro and Mattay, 1981). In this case the substitution of deuterium (D) for hydrogen (H) in the methyl groups of DPMP led to the results shown in Fig. 22. The cage effect for formation of methylstyrene and benzaldehyde is significantly affected by the substitution of D for [1]H.
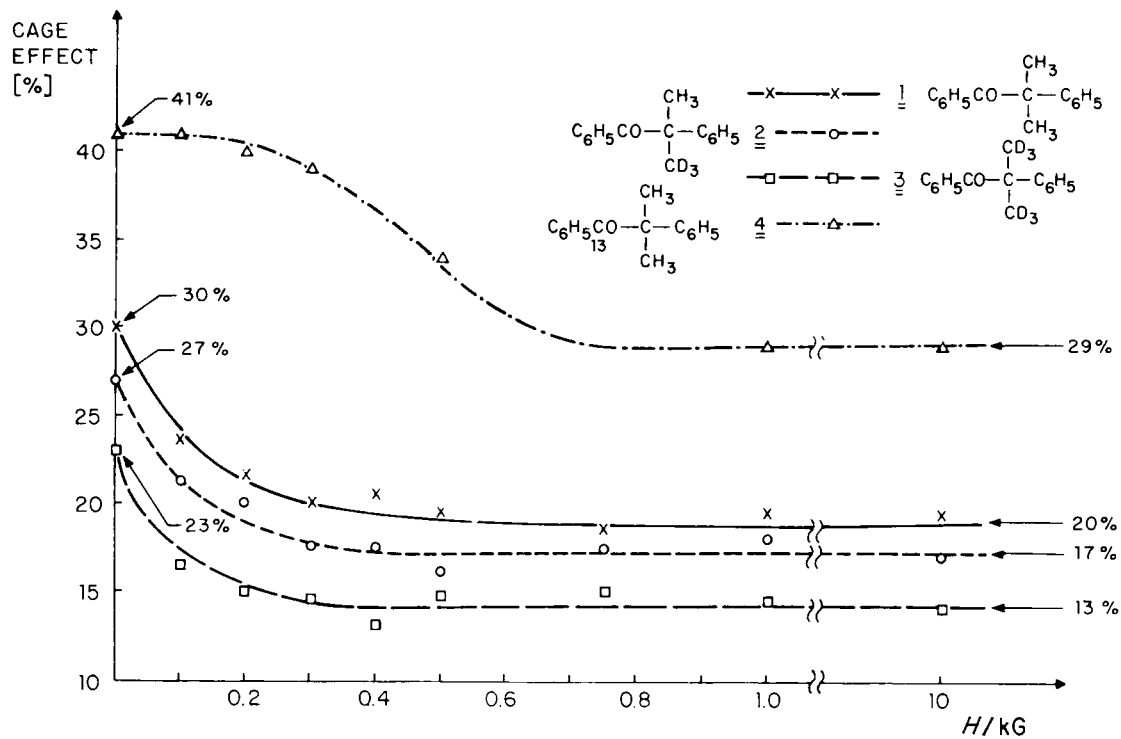
FIG. 22   Percentage cage effect as a function of applied field for variously isotopically substituted DPMP's

In particular it should be noted that substitution of CD_3 for CH_3 in DPMP reduces the cage effect from 30% to 23%. A check of the kinetic isotope effect on the atom transfer in the disproportionation reaction was made for $PhCOC(CH_3)(CD_3)Ph$. The H/D abstraction ratio was 1 : 1 as is typical for disproportionation reactions. Note also that ^{13}C substitution at the carbonyl carbon *increases* the cage effect from 30% to 41%. These results are readily explained in terms of a magnetic isotope effect since the smaller magnetic moment of D compared with H will cause a *slower* inter-system crossing rate in radical pairs possessing CD_3 groups relative to CH_3 groups, while the magnetic ^{13}C nuclei cause a more rapid intersystem crossing in radical pairs than the non-magnetic ^{12}C nuclei (Scheme 11). The slower
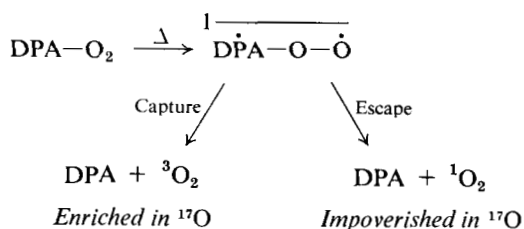

^{13}C increases intersystem crossing relative to ^{12}C

D decreases intersystem crossing relative to H
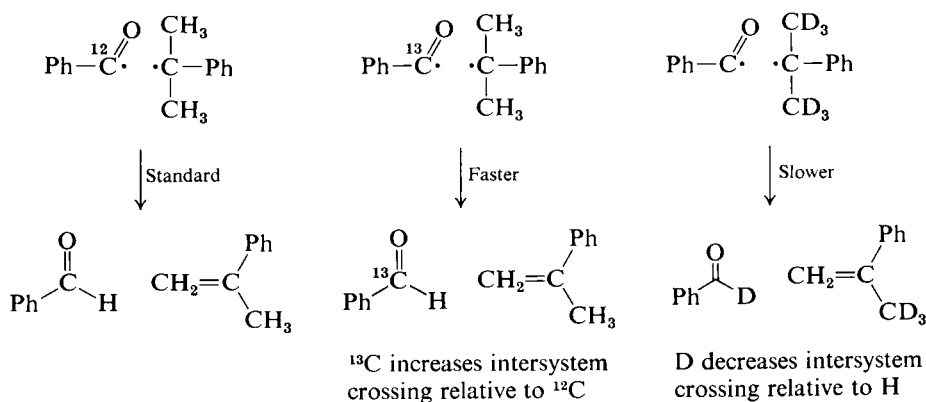
Scheme 11

intersystem crossing in the D/H case and the faster intersystem crossing in the $^{13}C/^{12}C$ case lead to a smaller and larger cage effect for the isotopically substituted compounds relative to DPMP. The strong magnetic field effect on the cage effects for the substituted compounds provides convincing evidence that the isotope effect is magnetic in origin.

Magnetic isotope effects involving oxygen nuclei

An example of a magnetic isotope effect involving ^{17}O has been demonstrated to occur in the thermolysis of endoperoxides of aromatic compounds (Turro and Chow, 1980). As discussed above, the decomposition of certain endoperoxides produces singlet molecular oxygen and the yield of singlet oxygen is magnetic field dependent (Fig. 15). These results were interpreted in terms of a diradical mechanism (Scheme 7) in which intersystem crossing of an initially produced diradical (^1D) to a triplet diradical (^3D) competes with decomposition of ^1D to yield singlet molecular oxygen. This scheme has

the elements needed for a magnetic isotope effect with the $^1D \rightarrow {}^1O_2$ process serving as an escape pathway for ^{16}O and ^{18}O nuclei (Scheme 12).

$$DPA-O_2 \xrightarrow{\lambda} {}^1\overline{D\dot{P}A-O-\dot{O}}$$

Capture / \ Escape

$$DPA + {}^3O_2 \qquad\qquad DPA + {}^1O_2$$

Enriched in ^{17}O *Impoverished in* ^{17}O

Scheme 12

To test the validity of these ideas, the thermolysis of the endoperoxide of 9,10-diphenylanthracene (DPA-O_2) was conducted in the presence of a selective and quantitative $^1O_2$ trap. The reaction of $^1O_2$ with the trap makes escape irreversible. It was found that ^{17}O-enriched DPA-O_2 produced less $^1O_2$ than DPA-O_2 containing ^{16}O or ^{18}O. Furthermore, the ^{17}O atoms proceed through the capture pathway to ^3D which decomposes to yield $^3O_2$ as an irreversibly formed product. Thus, the ^{17}O atoms are "captured" in the $^3O_2$ product. Measurement of the isotopic composition of the $^3O_2$ produced in the thermolysis revealed a substantial enrichment in ^{17}O content relative to that in DPA-O_2 (Table 6). The enrichment was strongly suppressed when the

TABLE 6

Yield of $^1O_2$ formation for thermolysis of DPA-O_2 and isotopic composition for thermolysis of ^{17}O-enriched DPA-$O_2{}^a$

Yield of $^1O_2{}^b$			Composition of ^{17}O in untrappable O_2	Solvent	Magnetic field
DPA-$^{16}O_2{}^c$	DPA-$^{17,18}O_2{}^d$	DPA-$^{18}O_2{}^e$			
0.37 ± 0.02	0.34 ± 0.01	0.37 ± 0.01	0.380 ± 0.005	CHCl$_3$	0.5 kG
0.32 ± 0.01	0.31 ± 0.01	0.31 ± 0.01	0.368 ± 0.002	CHCl$_3$	10 kG
			0.369 ± 0.001	CHCl$_3$	Control^f
0.32 ± 0.01	0.28 ± 0.02	0.32 ± 0.02	0.376 ± 0.001	Dioxan	0.5 kG
0.27 ± 0.02	0.23 ± 0.01	0.28 ± 0.02	0.376 ± 0.002	Dioxan	12 kG

[a] Turro and Chow, 1980
[b] Yield of $^1O_2$ is related to the consumption of a $^1O_2$ trap
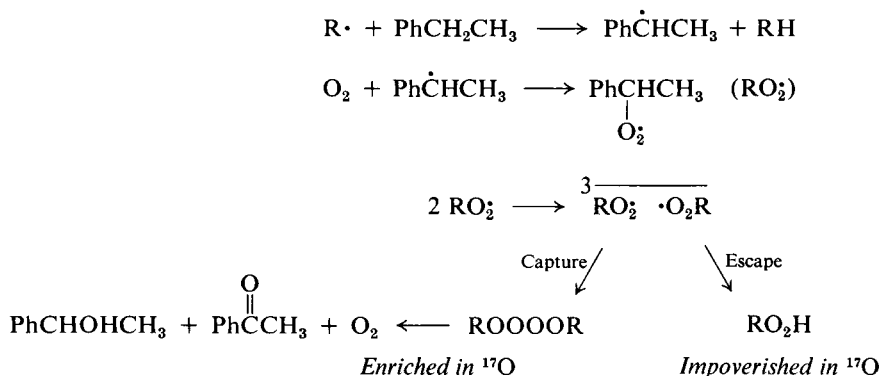[c] Initial composition is 99.8% ^{16}O
[d] Initial composition is 60% ^{18}O; 37% ^{17}O; (and 3% ^{16}O)
[e] Initial composition is 92% ^{18}O; 4% ^{17}O; (and 4% ^{16}O)
[f] Thermolysis of DPA-O_2 in the absence of a $^1O_2$ trap

endoperoxide thermolyses were performed in the presence of a strong magnetic field.

A radical-pair system for enrichment of ^{17}O *via* the magnetic isotope effect (Scheme 13) has been demonstrated (Belyakov *et al.*, 1978). The system takes advantage of interesting chemistry in the liquid-phase chain oxidation
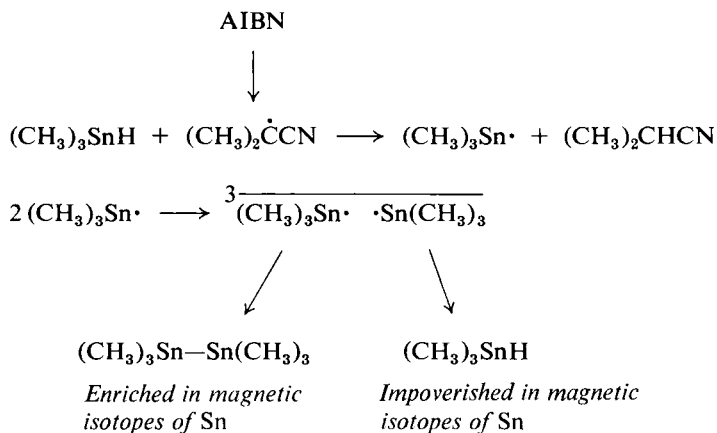
$$R\cdot + PhCH_2CH_3 \longrightarrow Ph\overset{\cdot}{C}HCH_3 + RH$$

$$O_2 + Ph\overset{\cdot}{C}HCH_3 \longrightarrow PhCHCH_3 \quad (RO_2^{\cdot})$$
$$\underset{\displaystyle O_2^{\cdot}}{\mid}$$

$$2\,RO_2^{\cdot} \xrightarrow{\quad} {}^{3}\overline{RO_2^{\cdot}\ \cdot O_2R}$$

Capture ↙   ↘ Escape

$$PhCHOHCH_3 + Ph\overset{O}{\overset{\|}{C}}CH_3 + O_2 \longleftarrow ROOOOR \qquad\qquad RO_2H$$

Enriched in ^{17}O *Impoverished in* ^{17}O

Scheme 13

of organic compounds. These oxidations proceed by the formation of peroxy radicals (RO_2) which terminate (at least in part) by radical pair combinations to form unstable tetraoxides (RO_4R) (Howard, 1972; Bennett and Howard, 1973). The latter spontaneously decompose to yield molecular oxygen and organic fragments. A magnetic isotope effect can occur at the stage of radical-pair formation. The random encounter of two RO_2 radicals is expected to produce three triplet radical pairs for each singlet radical pair (statistics of the spin states). The singlet radical pairs that are formed will probably combine to form RO_4R without any magnetic isotope effect, but the triplet radical pairs will behave as triplet correlated radical pairs and cage reaction will be more efficient for radical pairs containing magnetic isotopes (e.g. ^{17}O).

Going back to Scheme 13, RO_4R and the molecular oxygen and organic fragments found in RO_4R decomposition will be enriched in ^{17}O if a magnetic isotope effect occurs for the triplet $RO_2\cdot\cdot O_2R$ radical pair. Experimentally, the radical-initiated oxidation of ethylbenzene was conducted in a closed volume which allowed for the exchange of O_2 between the gas and liquid phases. As the oxidation proceeded, the initial molecular oxygen is consumed and ^{17}O enriched molecular oxygen is produced. Thus, as the reaction proceeds, the residual molecular oxygen becomes enriched in ^{17}O. An enrichment of 13% was found (*c.* 90% consumption of molecular oxygen), whereas the extent of enrichment in ^{18}O was negligible (see also Buchachenko *et al.*, 1984).

Magnetic isotope effects with tin

Naturally occurring tin is found in numerous isotopic forms, the most abundant of which are non-magnetic ([116]Sn, 14.3%; [118]Sn, 24%; [120]Sn, 33%; [124]Sn, 6%), but several of which are magnetic ([115]Sn, 0.35%; [117]Sn, 7.7%; and [119]Sn, 8.7%) and of spin 1/2.

Applying the general scheme for magnetic isotope enrichment, the system shown in Scheme 14 was investigated (Podoplelov *et al.*, 1979). In this case,

$$\text{AIBN}$$

$$\downarrow$$

$$(CH_3)_3SnH + (CH_3)_2\overset{\cdot}{C}CN \longrightarrow (CH_3)_3Sn\cdot + (CH_3)_2CHCN$$

$$2\,(CH_3)_3Sn\cdot \longrightarrow {}^3\overline{(CH_3)_3Sn\cdot \;\;\cdot Sn(CH_3)_3}$$

$$\swarrow \qquad\qquad \searrow$$

$$(CH_3)_3Sn-Sn(CH_3)_3 \qquad\qquad (CH_3)_3SnH$$

Enriched in magnetic   *Impoverished in magnetic*
isotopes of Sn   *isotopes of* Sn

Scheme 14

the electron spins of the radical pairs, which are produced from random free radicals, are determined by the statistics of the singlet and triplet states (1/4 and 3/4, respectively). The singlet pairs are expected to combine without regard to magnetic effects, but the triplet pairs are expected to follow the general rules for the case of initially correlated triplet radical pairs. Thus, the radical pair combination product is enriched in magnetic tin isotopes (16.0% initial; 17.8% final), whereas the free radical product was impoverished in magnetic tin isotopes (16.0% initial; 13.5% final). The enrichment (impoverishment) was found to depend on the concentration of reagents.

Other hetero-organic radicals (containing silicon, lead, etc.) also possess high values of hyperfine coupling constants (Harris and Mann, 1978). Thus, radical reactions involving hetero-organic compounds are candidates for separation of magnetic heteroatomic isotopes from their non-magnetic counterparts.

3 Conclusion

The crucial requirements for the observation of magnetic effects on chemical reactions may be summarized as follows:

1 An intermediate in which exchange interactions are sufficiently small as to allow intersystem crossing and thus production of a different spin state for the intermediate.

2 A reaction of the intermediate which is in competition with the magnetic field influenced intersystem crossing process, which enables a sorting of the reaction products of the different spin states of the intermediate to take place.

3 A proper balance of the rates of the intersystem crossing, electron exchange and the competition processes.

As we have seen, the competition process is almost exclusively the diffusive separation of the intermediate radical (ion) pair. Diffusive separation, together with the intersystem crossing process, controls the yield of cage products for radical pair reactions. For systems in which hyperfine interactions are dominant, the application of an external magnetic field either increases (for initially singlet radical pairs) or decreases (initially triplet radical pairs) the amount of cage reaction. For systems with a large value of Δg, the opposite effect may be observed.

The observations of external magnetic field effects on chemical reactions have been confined to changes in the distributions of reaction products, compared to those obtained for reactions performed in the earth's magnetic field. At first sight this may not appear to be a dramatic change in the reactivity of the system. However, it is important to realize that the product distribution reflects the dynamic behaviour of the intermediate radical pairs. If the changes in the dynamic properties of the radical pairs can be harnessed, then more dramatic effects may be observed in secondary processes. For example, the work of Turro on the photoinitiated emulsion polymerization of styrene has demonstrated that changes in the product polymer weight by a factor of five can be achieved by using a magnetic field which produces changes in the energy of the participating radicals of only $c.$ 10^{-4} kcal mol^{-1}.

In summary, a large number of well-documented examples of the magnetic field effect on chemical reactions exist. These effects have been observed in many different kinds of chemical systems, and are readily interpreted in terms of the well established principles of chemically induced magnetic polarization.

Acknowledgements

References

Atkins, P. W. (1970). "Molecular Quantum Mechanics". Oxford University Press, London

Atkins, P. W. (1973). *Chem. Phys. Lett.* **18**, 355
Atkins, P. W. (1976). *Chem. Brit.* 214
Atkins, P. W. and Lambert, T. P. (1975). *Ann. Rep. Prog. Chem.* **A72**, 67
Baretz, B. H. and Turro, N. J. (1983). *J. Am. Chem. Soc.* **105**, 1309
Bellamy, F. and Streith, J. (1976). *Heterocycles* **4**, 1391
Belyakov, V. A., Maltsev, V. I., Galimov, E. M. and Buchachenko, A. L. (1978). *Proc. Russ. Acad. Sci.* **243**, 561
Bennett, J. E. and Howard, J. A. (1973). *J. Am. Chem. Soc.* **95**, 4008
Berndt, A., Fischer, H. and Paul, H. (1977). "Magnetic Properties of Free Radicals". Landolt-Börnstein, New Series, Vol. 9b, Springer Verlag, Berlin
Bernstein, R. B. (1952). *J. Phys. Chem.* **56**, 893
Bernstein, R. B., (1957). *Science* **126**, 119
Buchachenko, A. L. (1976). *Russ. Chem. Rev.* **45**, 761
Buchachenko, A. L. (1977). *Russ. J. Phys. Chem.* **51**, 1445
Buchachenko, A. L. and Zhidomirov, F. M. (1971). *Russ. Chem. Rev.* **40**, 801
Buchachenko, A. L., Tarasov, V. F. and Maltsev, V. I. (1981). *Russ. J. Phys. Chem.* **55**, 936
Buchachenko, A. L., Fedorov, A. V., Yasina, L. L. and Galimov, E. M. (1984). *Chem. Phys. Lett.* **103**, 405
Carrington, A. and McLauchlan, K. A. (1967). "Introduction to Magnetic Resonance". Harper and Row, New York
Chung, C.-J. (1982). Ph.D. Dissertation, Columbia University, USA
Closs, G. L. (1971). *Proc. XXIIIrd Congr. Pure Appl. Chem.* **4**, 19
Duncan, J. F. and Cook, G. B. (1968). "Isotopes in Chemistry". Clarendon Press, Oxford, U.K.
Engel, P. S. (1970). *J. Am. Chem. Soc.* **92**, 6074
Fendler, E. J. and Fendler, J. H. (1975). "Catalysis in Micellar and Macromolecular Systems". Academic Press, London and New York
Frith, P. G. and McLauchlan, K. A. (1975). *Ann. Rep. Prog. Chem.* 378
Gupta, A. and Hammond, G. S. (1972). *J. Chem. Phys.* **57**, 1789
Harris, R. H. and Mann, B. E. (1978). "NMR and the Periodic Table". Academic Press, London and New York
Hata, N. (1976) *Chem. Lett.* 547
Hata, N. (1978). *Chem. Lett.* 1359
Hata, N. and Hokawa, M. (1981). *Chem. Lett.* 507
Hata, N., Ono, Y. and Nakagawa, F. (1979). *Chem. Lett.* 603
Howard, J. A. (1972). *Adv. Free Radical Chem.* **4**, 49
Kaptein, R. (1975). *Adv. Free Radical Chem.* **5**, 381
Kaptein, R., (1977). *In* "Chemically Induced Magnetic Polarization" (L. T. Muus, ed.). Reidel, Dordrecht, p. 1
Lawler, R. G. (1972). *Ace. Chem. Res.* **5**, 25
Lawler, R. G. and Evans, G. T. (1971). *Ind. Chim. Belg.* **36**, 1087
Leshina, T. V., Salikhov, K. M., Sagdeev, R. Z., Belyaeva, S. G., Maryasova, V. I., Purtov, P. A. and Molin, Y. N. (1980). *Chem. Phys. Lett.* **18**, 355
Molin, Y. N., Sagdeev, R. Z. and Salikhov, K. M. (1979). *In* "Soviet Scientific Reviews. Chemistry", Vol. 1. O.P.A., Amsterdam, Ch. 1
Podoplelov, A. V., Leshina, T. V., Sagdeev, R. Z., Molin, Y. N. and Goldanskii, V. I. (1979). *JETP Lett.* **29**, 380
Rigaudy, J. and Basselier, J. J. (1971). *Pure Appl. Chem.* **1**, 383
Sagdeev, R. Z., Molin, Y. N., Salikhov, K. M., Leshina, T. V., Kamha, M. A. and Shein, S. M. (1973a). *Org. Mag. Res.* **5**, 599

Sagdeev, R. Z., Molin, Y. N., Salikhov, K. M., Leshina, T. V., Kamha, M. A. and Shein, S. M. (1973b). *Org. Mag. Res.* **5**, 603

Sagdeev, R. Z., Leshina, T. V., Kamkha, M., Belchenko, O. I., Molin, Y. N. and Rezvukhin, A. L. (1977a). *Chem. Phys. Lett.* **48**, 89

Sagdeev, R. Z., Salikhov, K. M. and Molin, Y. N. (1977b). *Russ. Chem. Rev.* **46**, 297

Sakaguchi, Y., Hisahara, H. and Nagakura, S. (1980). *Bull Chem. Soc. Jpn.* **53**, 39

Sterna, L., Ronis, D., Wolfe, S. and Pines, A. (1980). *J. Chem. Phys.* **73**, 5493

Tanimoto, Y., Hayashi, H., Nagakura, S. and Tokumaru, K. (1976). *Chem. Phys. Lett.* **41**, 267

Tarasov, V. F., Buchachenko, A. L. and Maltsev, V. I. (1981). *Russ. J. Phys. Chem.* **55**, 1095.

Turro, N. J. (1978a). "Modern Molecular Photochemistry". Benjamin/Cummings, Menlo Park, p. 275

Turro, N. J. (1978b). *Ibid.*, p. 473

Turro, N. J. (1981). *Pure Appl. Chem.* **53**, 259

Turro, N. J. (1983). *Proc. Natl. Acad. Sc. (USA)* **80**, 609

Turro, N. J. and Cherry, W. R. (1978). *J. Am. Chem. Soc.* **100**, 7431

Turro, N. J. and Chow, M.-F. (1979). *J. Am. Chem. Soc.* **101**, 3701

Turro, N. J. and Chow, M.-F. (1980). *J. Am. Chem. Soc.* **102**, 1190

Turro, N. J. and Kraeutler, B. (1980). *Acc. Chem. Res.* **13**, 369

Turro, N. J. and Kraeutler, B. (1982). *In* "Diradicals". (W. T. Borden, ed.). Wiley, New York

Turro, N. J. and Mattay, J. (1981). *J. Am. Chem. Soc.* **103**, 4200

Turro, N. J., Chow, M.-F. and Rigaudy, J. (1979a). *J. Am. Chem. Soc.* **101**, 1300

Turro, N. J., Kraeutler, B. and Anderson, D. R. (1979b). *J. Am. Chem. Soc.* **101**, 7435

Turro, N. J., Chow, M.-F., Chung, C.-J. and Tung, C.-H. (1980a). *J. Am. Chem. Soc.* **102**, 7391

Turro, N. J., Chow, M.-F., Chung, C.-J., Weed, G. C. and Kraeutler, B. (1980b). *J. Am. Chem. Soc.* **102**, 4843

Turro, N. J., Gratzel, M. and Braun, A. M. (1980c). *Angew. Chem. Int. Ed. Engl.* **19**, 675

Turro, N. J., Anderson, D. R., Chow. M.-F., Chung, C.-J. and Kraeutler, B. (1981a). *J. Am. Chem. Soc.* **103**, 3892

Turro, N. J., Chow, M.-F., Chung, C.-J. and Kraeutler, B. (1981b). *J. Am. Chem. Soc.* **103**, 3886

Turro, N. J., Chung, C.-J., Jones, G. and Becker, W. G. (1982a). *J. Phys. Chem.* **86**, 3677

Turro, N. J., Chung, C.-J., Lawler, R. G. and Smith, W. J. (1982b). *Tetrahedron Lett.* 3223